

1 Even-Order Harmonic Distortion Observations during Multiple

2 Geomagnetic Disturbances: Investigation from New Zealand

3 Malcolm Crack and Craig J. Rodger

4 Department of Physics, University of Otago, Dunedin, New Zealand

5 Mark A. Clilverd

6 British Antarctic Survey (UKRI-NERC), Cambridge, United Kingdom

7 Daniel H. Mac Manus

8 Department of Physics, University of Otago, Dunedin, New Zealand

9 Ian Martin and Michael Dalzell

10 Transpower New Zealand Limited, New Zealand

11 Soren P. Subritzky and Neville R. Watson

12 Department of Electrical and Computer Engineering, University of Canterbury, Christchurch, New Zealand

13 Tanja Petersen

14 GNS Science, New Zealand

15

16 **Main point # 1:** A decade of even-order harmonic distortion data are used to investigate the

17 impact of space weather on a power network.

18 **Main point # 2:** In New Zealand four key substations containing single phase transformers act as

19 sources of enhanced harmonic distortion.

20 **Main point # 3:** The harmonic distortion is found to propagate into the nearby power network

21 over 150-200 km distances, decaying at a rate of $-0.0043 \text{ \%km}^{-1}$.

22

23 **Abstract.** Large geomagnetic storms are a space weather hazard to power transmission
24 networks due to the effects of Geomagnetically Induced Currents (GICs). GIC can
25 negatively impact power transmission systems through the generation of even-order current
26 and voltage harmonics due to half-cycle transformer saturation. This study investigates a
27 decade of even-order voltage total harmonic distortion (hereon referred to as ETHD)
28 observations provided by Transpower New Zealand Ltd., the national system operator. We
29 make use of ETHD measurements at 139 locations throughout New Zealand, monitored at
30 377 separate circuit breakers, focusing on 10 large geomagnetic disturbances during the
31 period 2013-2023. Analysis identified 5 key substations, which appeared to act as sources
32 of ETHD. The majority of these substations include single phase transformer banks, and
33 evidence of significant GIC magnitudes. The ETHD from the source substations was found
34 to propagate into the surrounding network, with the percentage distortion typically decaying
35 away over distances of 150-200 km locally, i.e., at a rate of $-0.0043 \text{ \% km}^{-1}$. During the
36 study period some significant changes occurred in the power network, i.e., removal of the
37 Halfway Bush single phase bank transformer T4 in November 2017, and decommissioning
38 of the New Plymouth substation in December 2019. Decommissioning of these two assets
39 resulted in less ETHD occurring in the surrounding regions during subsequent geomagnetic
40 storms. However, ETHD still increased at HWB with increasing levels of GIC, indicating
41 that three phase transformer units were still susceptible to saturation, albeit with about 1/3
42 of the ETHD percentage exhibited by single phase transformers.

43
44 **Plain Language Summary.** Space weather, triggered by solar storms, can lead to
45 significant variations in the Earth's magnetic field.. The magnetic variations are termed
46 geomagnetic disturbances. Changing magnetic fields induce electric fields at the Earth's
47 surface, causing unwanted currents to flow in electrical power transmission networks. These
48 Geomagnetically Induced Currents (GICs), pose a hazard to network operations as they can

49 cause networks to become destabilized, leading to blackouts and damage to transformers.
50 One negative impact of GIC in a power network is the production of harmonics of the
51 power transmission frequency (typically 50 or 60 Hz); such harmonics contributed to the
52 blackout of the Québec power system in March 1989. In our paper we study harmonic
53 distortion occurrence in the New Zealand power grid using measurements from 139
54 substations across the country during 10 geomagnetic storms. Analysis identified 5 key
55 substations, which appeared to act as sources of harmonic distortion. The majority of these
56 substations include a particular transformer design which is known to be more susceptible
57 to GIC issues, as well as evidence of significant GIC.

58

59

60

61 **1. Introduction**

62 In recent years there has been growing interest from policy makers around the hazards posed
63 by Space Weather to our deeply technologically-connected society. One example is the report
64 from UN Committee on the Peaceful Uses of Outer Space [*United Nations*, 2017]. They
65 noted that "The largest potential socioeconomic impacts arise from space weather driven
66 geomagnetically induced currents in electrical power networks". This comment flows from
67 hardware in electrical power transmission systems being disrupted, in some cases even
68 permanently damaged, during significant geomagnetic storms that have occurred during the
69 last 3 decades (approximately). This has occurred over a wide range of countries, with
70 examples being Canada, New Zealand, Norway, South Africa, Sweden, and the United States
71 of America.

72
73 The most extreme example of such a disruption occurred in the Canadian province of
74 Québec during a geomagnetic disturbance (GMD) in 13-14 March 1989, where the power
75 network was rapidly destabilized leading to a very wide-scale and long-lasting blackout
76 [*Béland and Small*, 2004; *Guillon et al.*, 2016]. In modern societies, reliable electricity supply
77 is vital. An extreme storm, expected to produce much larger GMD, is likely to collapse the
78 electrical power grid in many locations across the world [e.g., *JASON*, 2011; *Baker et al.*,
79 2008; *Oughton et al.*, 2017; *Mac Manus et al.*, 2022b]. The flow-down impacts from a major
80 disruption are likely extreme and far reaching. Electrical power supply is the life-blood of
81 modern economic and social systems. Disruptions will include extensive societal and
82 economic impacts from loss of electrical power for essential services, businesses, and
83 households.

84

85

86

87 Geomagnetically Induced Currents can adversely affect electrical power infrastructure
88 through disruption to operations or hardware damage through multiple different routes [e.g.,
89 *Samuelsson, 2013; Boteler, 2015*], leading to system instabilities that can produce a voltage
90 collapse and blackout. One of these routes is from harmonic distortion to the alternating
91 current (AC) waveform due to saturated power grid transformers. The GIC, being quasi-
92 direct current (DC), produces half-cycle saturation in transformers, leading to increased
93 audible noise and excessive heating of transformers. Saturated transformers dissipate large
94 quantities of power and also generate harmonics. The consequences of these impacts are
95 incorrect operation of protective relays, voltage dips, changes in power flow, and possible
96 system frequency shifts [*EPRI, 1983*]. It is clear that GIC-produced harmonic distortion
97 contributed significantly to the Hydro Québec blackout in 1989 [*Guillon et al., 2016*].

98

99 It is important to note how GIC causes asymmetric saturation and the production of
100 harmonics (see, for example *Arrillaga and Watson [2003]*). When a transformer is subjected
101 to higher than its rated AC voltage the peak magnetic flux can exceed the transformer core
102 capabilities. This then leads to symmetric saturation and the production of odd-order
103 harmonic components. While unwanted, this is a common issue faced in the design and
104 operation of electrical power systems. In contrast, GIC provides a DC component in the
105 transformer windings such that the transformer core saturates in only one direction, termed
106 asymmetric saturation or "half-cycle" saturation. Because of the asymmetric nature of the
107 current, half-cycle saturation results in even- and odd-order harmonic components [e.g.,
108 *Boteler et al., 1989*].

109

110 While harmonic distortion is clearly an important route by which space weather can produce
111 hazards for electrical power networks, there is a limited amount of discussion and research

112 into this in the scientific literature. This may reflect, in part, difficulties researchers
113 experience in getting access to harmonic distortion data. At the same time, it appears that
114 harmonic distortion levels are commonly collected by power-grid operators to monitor
115 operations and power quality. In contrast, observations of GIC seem to be rare in most power
116 systems, making that dataset also very difficult to source for scientific research. The
117 importance of this was emphasized in a recent study of changing harmonic distortion levels
118 and GIC observations during two GMD in New Zealand [Rodger *et al.*, 2020]. Those authors
119 stated: "We hence emphasize that GIC leading to asymmetric transformer saturation is one of
120 the few ways to produce even harmonics, and as such even-order harmonic measurements
121 should be a very valuable route to study space weather impacts on power networks". That
122 comment is supported by the response of Hydro-Québec to the March 1989 blackout. Hydro-
123 Québec introduced multiple monitoring systems to assist the system operators, including:
124 real-time monitoring and control centre reporting of voltage harmonics (9 substations), real-
125 time monitoring and control centre reporting of even harmonic distortion at (4 substations),
126 and offline monitoring of voltage and current harmonics plus DC GIC observations (5
127 substations) [Guillon *et al.*, 2016].

128

129 Over roughly the last decade, the mid-latitude south Pacific country of New Zealand has
130 proved to be a valuable "laboratory" for studies into space weather GIC impacts. New
131 Zealand is one of the few countries that have already experienced direct transformer damage
132 from a large geomagnetic storm, with a transformer damaged beyond repair at the Halfway
133 Bush substation in Dunedin after the 6 November 2001 GMD [Béland and Small, 2004;
134 Marshall *et al.*, 2012; Mac Manus *et al.*, 2017]. New Zealand is unusual in that there is a
135 long-lasting and relatively dense network of DC GIC observations available in parts of that
136 country [Mac Manus *et al.*, 2017; Rodger *et al.*, 2020], with power grid operator staff willing
137 and interested to collaborate with local researchers. The DC observations were originally

138 deployed to monitor the operation of the high voltage DC link between New Zealand's main
139 islands (see the discussion in *Mac Manus et al.* [2017]), but the network is now being
140 expanded to include space weather monitoring. All the real time DC observations are
141 available in the system operations control room, and operational procedures have been
142 developed to try to mitigate GIC impact during a GMD [*Transpower*, 2015; *Mac Manus et*
143 *al.*, 2023]. The New Zealand GIC data has allowed efforts to better investigate GIC drivers
144 [*Mac Manus et al.*, 2017], empirical estimates of likely extreme GIC magnitudes [*Rodger et*
145 *al.*, 2017; *Ingham et al.*, 2017], and to show that GIC levels differ in the same storm between
146 transformers in the same substation due to resistance differences between transformers and
147 connections [*Divett et al.*, 2018]. Access to observation data, both GIC and detailed network
148 layouts and resistances, have allowed theoretical modeling of time-varying GIC amplitudes at
149 the transformer level to be developed [*Divett et al.*, 2017; *Divett et al.*, 2018; *Mukhtar et al.*,
150 2020; *Mac Manus et al.*, 2022a]. This has recently culminated in an estimation of extreme
151 storm GIC levels for a set of Carrington-storm level scenarios [*Mac Manus et al.*, 2022b]
152 using the validated modeling, which found that there are at risk transformers across the
153 country including major population centers at the northern and southern extremes of the
154 country. These Carrington-storm level GIC scenarios have provided the basis of new
155 mitigation planning [*Mac Manus et al.*, 2023], producing a new operational space weather
156 mitigation plan for the New Zealand power grid operator, Transpower New Zealand Ltd.

157

158 Transpower New Zealand also undertakes regular monitoring of harmonic distortion, and
159 has provided observations for local space weather research. The harmonic distortion power
160 quality measurements have comparatively low time resolution (10 min averages), but can still
161 provide insights. A detailed examination of harmonic production in the Halfway Bush
162 substation in Dunedin during the GMD of 7-8 September 2017 has been undertaken
163 combining GIC measurements at that substation, magnetic field variations, and harmonic

164 distortion observations made at both low time resolution by Transpower power quality
165 monitoring systems and also at very high time resolution using a co-located VLF wideband
166 radio receiver [Clilverd *et al.*, 2018, 2020]. These studies confirmed that high GIC lasting
167 significant time periods (i.e., several minutes) produced clear increases in even-order
168 harmonics, while higher but more short-lived GIC events produced no evidence of harmonic
169 production. This is consistent with high averaged GIC levels leading to transformer saturation
170 and even-order harmonic production, as expected from asymmetric saturation. *Rodger et al.*
171 [2020] expanded on that work, examining even-order voltage harmonic distortion
172 measurements made at 377 circuit breakers at 126 separate locations across both the North
173 and South Island of New Zealand. That analysis showed that increased even-order voltage
174 harmonic distortion occurred where there were significant GIC magnitudes which lasted over
175 long time periods, consistent with the earlier findings for the single substation reported by
176 *Clilverd et al.* [2018, 2020]. However, these 126 location observations also demonstrated
177 how GIC effects could be identified in even-order harmonic distortion monitoring for
178 locations where no in-situ GIC measurements were present (for example, the upper South
179 Island or the majority of the North Island). This included substations in the northern part of
180 the province of Taranaki in the North Island of New Zealand, a location approximately
181 corresponding to Luxembourg City (Luxembourg) in Europe or Memphis (Tennessee) in
182 North America.

183

184 In the current study we expand on the earlier work of *Rodger et al.* [2020] to examine
185 multiple GMD and harmonic distortion observations across the New Zealand power
186 transmission network. We also contrast the substation locations in New Zealand expected to
187 have high GIC in an extreme GMD [*Mac Manus et al.*, 2022b] with even-order voltage
188 harmonic distortion observed during recent GMD.

189

190 **2. Experimental Datasets**

191 **2.1 New Zealand National Grid and GIC Observations**

192 The New Zealand national grid stretches across both the North Island and South Island, and
193 is made up of ~11,000 km of high-voltage overhead transmission lines and ~200 km of
194 underground cables, connecting 170 substations [*Transpower*, 2021]. The core high voltage
195 transmission network operates at 220 kV, with a secondary network of 110 kV transmissions
196 lines and a small amount of high voltage transmission at 66 kV to support smaller centres and
197 generation [*Mac Manus*, Fig. 5.9 and 5.11, 2023]. Due to New Zealand's geographical
198 location there are no connections to other countries power networks, unlike the situation in
199 much of the world. The North and South Island are only connected by the 1430 A high
200 voltage direct current link, operating at 350 kV, primarily used to bring hydro-electrically
201 generated power from the South Island to the more populated North Island.

202

203 A detailed description of the New Zealand GIC measurements in the South Island has been
204 previously reported [*Mac Manus et al.*, 2017] and updated [*Rodger et al.*, 2020]. The
205 following section is a very brief summary, and the reader is directed to the earlier studies for
206 a more complete explanation.

207

208 Transpower New Zealand Limited has measured DC currents in multiple transformer
209 neutral connections using Hall effect current transducers. These transducers are Liaisons
210 Electroniques-Mécaniques (LEM) model LT 500 or LT 505, with about half of each in use,
211 and a mix of -S and -T subtypes for both model cases. The primary purpose for the DC
212 observations is monitoring stray currents when the high voltage direct current (HVDC) link
213 between the South and North Islands operates in earth return mode or with unbalanced
214 currents on the conductors. For our purposes the LEM-provided DC measurements need to be
215 corrected to remove the HVDC stray currents as described by *Mac Manus et al.* [2017],

216 leaving only GIC. During GMD the typical LEM sampling rate is one measurement every
217 4 s. Due to the low time resolution of the harmonic distortion data, the GIC measurements
218 will typically be down-sampled to 10 minute averages, corresponding to the same time
219 window as the harmonic distortion data.

220

221 **2.2 New Zealand Harmonic Distortion Observations**

222 In this study we examine all even-order voltage total harmonic distortion observations made
223 by Transpower at circuit breakers in substations across New Zealand during a series of
224 selected GMD (described in Section 3). Harmonic distortion observations are made at the
225 majority of Transpower substations in New Zealand (i.e., transmission substations) using
226 Schneider PowerLogic ION8800 meters, which provide harmonic reporting up to the 63rd
227 harmonic on both voltage and current inputs. The meters are capable of providing total, even-
228 order, and odd-order harmonic recording. Transpower has provided us with power quality
229 measurements including the harmonic distortion observations with 10 minute time resolution
230 made at 477 circuit breakers at 139 substations (with the number depending on the time
231 period being considered). The locations of the harmonic distortion observations are shown in
232 Figure 1, and include 88 substations in the North Island and 55 in the South Island.
233 Measurements are available for most locations starting from near the end of 2013. The
234 database we used ran through to April 2022 (with specific substations downloaded to allow
235 analysis of GMD in early 2023, for which the observations were considered through to April
236 2023).

237

238 In Transpower's case the combined total, even, and odd-order harmonic distortion
239 percentages are archived from each meter on each of the three phases with a 10 min time
240 resolution. In the current study we focus only on the percentage distortion of the combination
241 of all even-order harmonics monitored on the circuit breaker voltage input, which we term

242 the ETHD. This decision was made after looking at the odd-THD observations, and finding
243 they did not seem to provide meaningful results linked to GMD; as expected following earlier
244 analysis [e.g., *Clilverd et al.*, 2018]. As noted in *Rodger et al.* [2020], voltage harmonic
245 distortion observed at a given monitoring location may not be locally generated, and is
246 influenced by other substations linked to the given monitoring location by transmission lines.
247 In contrast, current harmonic distortion observations provide a direct indication of the source
248 from which the harmonics originate. Unfortunately, the Transpower phase current THD
249 measurements do not discriminate between even and odd harmonics, but include both even
250 and odd harmonics.. As reported earlier, the total of both even and odd harmonic distortion
251 does not respond in a useful way during space weather events [*Clilverd et al.*, 2018; *Rodger*
252 *et al.*, 2020], and hence we restrict ourselves to the available even-order voltage THD (which
253 we now refer to as ETHD). The influence of nearby substations is discussed further in Section
254 4.

255
256 Each substation includes multiple circuit breakers (CB) for which ETHD measurements are
257 made, with separate measurements made on each of the 3 phases. In some locations there may
258 only be 1 monitored CB at a location, but the maximum number is 30 with an average of 3-4 CBs
259 monitored per substation location. Average ETHD values are provided for each phase at each CB
260 with 10 minute time intervals (i.e. 0-10, 10-20, 20-30, etc). The ETHD values are very similar
261 across the 3 phases, as expected for a balanced three-phase system, and thus we take the mean
262 of these values for each CB. *Rodger et al.* [2017] showed that the ETHD values could vary
263 inside the same substation, but with the same time variation; this may be due to attenuation
264 inside the substation linking different voltage levels. It is possible that this may be hidden in
265 substations with few CB, such that averaging might "downgrade" the importance of the ETHD
266 at a given substation. We therefore take the largest ETHD value amongst the CBs at a given

267 time; we typically find that the CB which exhibits the highest ETHD in a given substation
268 continues to show the highest ETHD over time during a GMD.

269

270 The process of taking the maximum ETHD value from the CBs in a given substation typically
271 provides good quality information, but at some locations this is not the case. In the vast majority
272 of New Zealand substations all the CB-ETHD values respond together, with only the magnitudes
273 differing. This is the typical situation during GMD. In some fairly rare cases we find times
274 unconnected with GMD where one or two CBs in a substation shows an ETHD increase, and the
275 remaining CBs do not. These ETHD increases do not influence nearby connected substations, as
276 is commonly seen during GMD (this is discussed more in Section 4). This type of non-GMD
277 ETHD increase was identified as occurring in a set of substations in the North island running
278 South to North and marked in the right hand panel of Figure 1 as white diamonds (from south to
279 north the substations shown are Bunnythorpe, Tangiwai, Taumarunui, Hamilton). On
280 consultation with Transpower we learnt that these substations provide special traction services to
281 the North Island Main Trunk electrified train services, and are thus different to the vast majority
282 of New Zealand substations; our Transpower engineering colleagues indicate that ETHD
283 increases occurring outside of GMD are most probably caused by rail operations near the
284 substation. Such events are not particularly common, and have not impacted the GMD analysis
285 described below. We note this effect, however, to emphasize that the situation is not quite as
286 simple as indicated by *Rodger et al.* [2020].

287

288 **2.3 New Zealand Magnetometer Observations**

289 GMD observations are provided by the sole magnetic observatory in New Zealand, the
290 Eyrewell (EYR) magnetometer operated by GNS Science, New Zealand. EYR is part of
291 INTERMAGNET (<http://www.intermagnet.org/>). A detailed description of the construction
292 of EYR one-minute averages of the horizontal component of the magnetic field, H , is given

293 in *Mac Manus et al.* [2017]. Due to the low time resolution of the harmonic distortion data,
294 the EYR horizontal magnetic field measurements will typically be averaged to 10 minute
295 resolution over the same time window as the ETHD data.

296

297 **2.4 Geomagnetic Disturbance (GMD) Events Examined**

298 Previous studies have shown that the rate of change of the horizontal component of the
299 magnetic field (H') was a good proxy for the observed GIC magnitude in New Zealand [e.g.,
300 *Mac Manus et al.*, 2017], using measurements from the Eyrewell observatory. *Rodger et al.*
301 [2020] also showed that the time variation of the 10 minute averaged Eyrewell H' provided
302 some indication of the time varying ETHD magnitudes across New Zealand. Based on this
303 we selected a set of GMD using the EYR H' observations across the time window for which
304 we have access to ETHD measurements. These GMD times are given in Table 1, which also
305 includes the peak absolute horizontal rate of change measurements from EYR ($|H'|$) at both 1-
306 minute and 10-minute time resolutions. Note there are other GMD which occurred during this
307 time period which are not given in Table 1. That occurs due to missing data; there are a
308 handful of unfortunate occurrences when a significant GMD occurs during a nationwide gap
309 in THD data, for example during 22 June 2015.

310

311 Three of the most important GMD in Table 1 are those of September 2017 (peak $|H'|$ of
312 33 nT/min at 1 minute resolution), August 2018 (peak $|H'|$ of 43 nT/min), and November
313 2021 (peak $|H'|$ of 32 nT/min). These three storms are particularly useful because they have
314 some of the highest peak $|H'|$ values in our time frame, whilst also occurring at times in
315 between important changes to the power grid which impact our ETHD observations. They are
316 shown in bold in Table 1. These are 1). On the 21 November 2017 the earthed single-phase
317 Halfway Bush (HWB) transformer number 4 (HWB T4) was taken out of service. 2). On 20

318 December 2019 the New Plymouth (NPL) substation, which contained at least one earthed
319 single-phase transformer, was entirely decommissioned.

320

321 **3. Even-order Total Harmonic Distortion (ETHD) Variations**

322 Outside of GMD periods, we see no coherent large spatial scale ETHD variations. Indeed,
323 typically there are no significant ETHD changes in most locations. However, during a GMD
324 all CBs show increases with the same time variation and these often appear to influence
325 connected substations. As seen previously for September 2017 [*Rodger et al.*, 2020], during a
326 GMD there is a consistent ETHD time varying response across the vast majority of the
327 monitored substations. Another source of ETHD increases local to a substation comes from
328 spectral leakage from local ripple injection systems used to control domestic hot water
329 heating systems in the local area. Once again, this is seen to be independent of GMD and is
330 very localized, typically occurring at the same times of day over long time periods. There
331 appear to be some other sources of local ETHD "spikes", and also offsets. We have not found
332 they significantly detract from our GMD-focused analysis, and will mention work-arounds as
333 they are applied.

334

335 **3.1 Case Studies of Time Variations**

336 Figure 2 shows examples of ETHD changes for 2 of the GMD considered, at a number of
337 locations which show clear and strong responses in ETHD to GMD. The upper row of Figure
338 2 presents the rate of change of the horizontal component of the magnetic field measured at
339 EYR (blue line), converted to 10 min time resolution. The following three rows are
340 percentage ETHD changes (red lines) for 3 selected substations: Halfway Bush (HWB), New
341 Plymouth (NPL), and Robertson Street (ROB). The left hand column shows these variations
342 for a GMD in September 2017, while the right hand column is for August 2018. The plots

343 show there are typically strong correlations in the timing of changes in ETHD and EYR, with
344 some correlation also in the magnitude of those changes, i.e., a larger or smaller EYR 10 min
345 resolution H' value will tend to produce larger or smaller ETHD at the same time resolution.
346 However, it is not uncommon for the ETHD response to lag slightly behind the GIC
347 response. A sudden spike in GIC magnitude will typically be seen in the ETHD in the same
348 10 min time window, or in the ETHD observations in the 10 min period immediately
349 following the GIC spike. This is likely due to time delays between the GIC spike and
350 transformer core-saturation, which then produces ETHD.

351

352 The selected time periods and locations shown in Figure 2 are not the only locations in these
353 storms with notable harmonic activity. We see similar patterns in ETHD "hot-spots" during
354 other storms, with the amount of ETHD corresponding roughly to the level of geomagnetic
355 activity. As reported by *Rodger et al.* [2020], GMD produce ETHD increases in multiple
356 substations across the country. However, as will be shown below, the examination of multiple
357 GMD over a longer time period in which significant network changes occurred indicates
358 there is more complexity to the linkage that they reported.

359

360 **3.2 Baseline corrected New Zealand wide analysis**

361 As can be seen in Figure 2, in many locations there is a fluctuating baseline value for
362 ETHD, i.e., the values often do not sit at zero percent outside of quiet times. In many
363 locations a constant amount of ETHD is reported to be present, unrelated to GMD. These
364 values tend to be small, but as they are clearly not due to GMD, we undertake data processing
365 outlined below to remove these constant baselines. We speculate these baseline offsets are
366 due to ETHD measuring errors, as the production of ETHD is unusual in a well run power
367 network, as discussed in *Rodger et al.* [2019] (outside of the short time periods where
368 transformers are initially energized [*Watson and Arrillaga, 2018*]). However, it is also

369 possible that these locations include devices which only draw current on one half cycle of the
370 AC wave. One example are half wave rectifiers, which would produce a long term near
371 constant ETHD level. We also note that for a small number of substations the data quality is
372 not good, which was also pointed out by *Rodger et al.* [2020], where the baselines vary
373 considerably over time. There are several such locations in the central North Island
374 (particularly around the city of Rotorua), which we speculate may be linked to equipment in
375 the forestry and wood processing industry. Other examples where ETHD spikes unrelated to
376 GMD can be produced are passing trains (discussed earlier) and spectral leakage from ripple
377 control systems. During the manual inspection of ETHD around GMD periods these issues
378 were obvious, as they were rare and very different from the main ETHD-variation which was
379 clearly linked to GMD. Locations with such issues were excluded for further analysis, but the
380 issue is mentioned for completeness and to assist future researchers.

381

382 In order to remove the impact of non-zero ETHD baselines, and to allow a better "like with
383 like" comparison, our subsequent analysis is undertaken using ETHD percentage values after
384 the baseline is removed. This is undertaken separately for each substation and GMD. The
385 baseline is calculated as the mean ETHD value for a given substation for the time period of the
386 geomagnetic disturbance plus one day before and after the peak of the storm.

387

388 Figure 3 presents six example maps of the baseline-corrected ETHD values across New
389 Zealand near the peak GMD 10 min periods for three significant GMD: September 2017,
390 August 2018, and November 2021, i.e., 2 examples per GMD. For each substation, the radius
391 of the plotted ring is proportional to the magnitude of the baseline-corrected 10 min mean
392 ETHD percentage value, where the value plotted is from the CB with the maximum for that
393 substation (as discussed earlier). The time shown on each panel represents the end of the
394 10 min window over which the mean was taken. We use color to help discriminate between

395 ring sizes: increases between 0-0.1% in ETHD (blue), 0.1% to 0.3% ETHD (orange), and
396 >0.3% ETHD (red). Black markers represent ETHD responses which are below the base-line, or
397 no data. In each panel an additional subpanel is included which shows the time series of the
398 magnetic field changes ($|H'|$, blue line), and a vertical red line marking the point in time
399 corresponding to that map.

400

401 Figure 3 indicates that ETHD increases are seen in multiple locations in the South Island,
402 particularly in Dunedin, but are also seen in multiple locations across the lower South Island,
403 both north and south of Dunedin. ETHD increases are also seen in the South Island city of
404 Christchurch, and surrounding areas. We note that high GIC magnitudes have previously
405 been reported in both the Islington substations (Christchurch, particularly transformer number
406 6, i.e., ISL T6) [Marshall, *et al.*, 2012; Mac Manus *et al.*, 2017; Rodger *et al.*, 2017; Divett *et*
407 *al.*, 2018]. In addition, very high GIC has been reported in multiple transformers in the
408 Dunedin substations of Halfway Bush and South Dunedin [e.g., Mac Manus *et al.*, 2017;
409 Rodger *et al.*, 2017, Mac Manus *et al.*, 2022a]. This may, in part, help explain the significant
410 ETHD increases seen in the Dunedin region, north and south of that city, and also around
411 Christchurch. Significant ETHD increases are also seen in the Tasman/West Coast region of
412 the upper South Island, and around Taranaki in the western North Island. There are also
413 ETHD increases seen in New Zealand's biggest cities, Auckland and Wellington.

414

415 The middle panels of Figure 3 show baseline-corrected ETHD maps for two significant time
416 periods during the 26 August 2018 GMD. A set of three single phase transformers in Halfway
417 Bush, Dunedin (HWB T4), was decommissioned in November 2017, such that this GMD
418 occurs after the last single phase transformer bank set earthed on the high voltage side was
419 removed from Dunedin city. While high GIC are still observed in Dunedin city, at levels
420 similar to those earlier measured at HWB T4, the levels of ETHD across the lower South

421 Island are very different from that seen before HWB T4 was decommissioned. This single
422 change has led to a dramatic decrease in ETHD levels in that part of New Zealand, indicating
423 that HWB T4 might have been the source of much of that ETHD. Most of the other ETHD
424 enhancement regions identified in the upper panels during the September 2017 GMD,
425 particularly the West Coast of the South Island, Taranaki, and the Auckland region, are still
426 seen during the August 2018 GMD.

427

428 The lower panels of Figure 3 are maps during the November 2021 GMD. Once again, there
429 is another dramatic decrease in ETHD relative to the earlier maps. This GMD occurred after
430 the New Plymouth (NPL) substation was decommissioned in December 2019, removing
431 another set of single phase transformers. For the last GMD example there are, again, some
432 ETHD increases in the Dunedin region (but with little evidence across the lower South
433 Island), some increases on the West Coast of the South Island and small increases in the
434 Auckland region, but the dramatic feature on the North Island's west coast, Taranaki,
435 essentially disappears. This demonstrates the importance of single phase units to ETHD
436 production during these GMD, caused by that transformer type having lower GIC saturation
437 thresholds than for 3 phase transformers [Dong *et al.*, 2001; NERC, 2013; EPRI, 2014;
438 *Piccinelli and Krausmann*, 2015].

439

440 From Figure 3 we identify 5 key substations to examine in more detail, with each appearing
441 to be the primary generator of ETHD in their respective regions. These are Halfway Bush
442 (HWB), Islington (ISL), Robertson Street (ROB), New Plymouth (NPL), and Henderson
443 (HEN). Note that in the Auckland region it is challenging to decide which substation might
444 be the source of the ETHD observations. Henderson was selected as it was previously
445 identified as a location with high GIC in GMD modeling [Mac Manus *et al.*, 2022b], and also
446 because it contains multiple single phase transformers. We note that four of the five

447 substations named above appear in the high GIC substations based on modeling reported in
448 Figure 10 of *Mac Manus et al.* [2022b]. The exception is Robertson Street (ROB) on the
449 West Coast of the South Island. While this substation "stands out" in Figure 3, it has not been
450 previously identified as an expected high GIC substation; nor does it contain any single phase
451 transformers.

452

453 Table 2 summarizes the baseline-corrected ETHD response observed at each of the 5 key
454 substations, for each of the 10 GMD examined in detail. Once again, we show in bold the
455 three most significant GMD. A "yes" in the table indicates a clear ETHD response i.e., by eye
456 it is clear that ETHD at that substation responds to the GMD. "Unclear" means we are not
457 confident. This often means there was small ETHD increases correlated with the peak of the
458 storm which was not bigger than other ETHD increases occurring within ± 1 day which were
459 clearly not correlated with GMD. A "no" indicates nothing was seen, and "-" indicates no
460 data was available for that location during the GMD in question. As is clear from Table 2,
461 most of our substations of interest show clear ETHD increases for the selected GMD. Some
462 of the clearest exceptions to this statement is for HWB from 28 Feb 2019 onwards, after the
463 single phase transformers HWB T4 was decommissioned (November 2017), and for NPL
464 from 12 Oct 2021 onwards, after the entire substation was decommissioned. It is important to
465 note that the removal of HWB T4 has not stopped the occurrence of GMD-linked ETHD
466 increases, as seen in Figure 3 and Table 2. However, the ETHD increases are not as clear or
467 consistent since the removal of HWB T4.

468 **4. ETHD Propagation from Source Substations**

469 It appears that significant quantities of the GMD-ETHD increases are linked to well defined
470 sources, potentially one single phase transformer bank with high GIC in a single substation.
471 As noted earlier, voltage harmonics can propagate through a transmission network, allowing

472 ETHD produced in one substation to influence large regions. The dramatic decrease in GMD-
473 linked ETHD in the lower South Island after the removal of HWB T4, and ETHD in the mid
474 and lower western North Island after the decommissioning of NPL are both strongly
475 suggestive of single ETHD sources propagating over wide spatial zones.

476

477 **4.1 Comparison GMD-linked ETHD changes to network grounding**

478 Further evidence of significant propagation of voltage ETHD comes from the nature of the
479 substations in which GMD-linked ETHD are observed around the substations we suspect are
480 the sources. A good example is the increase of ETHD in the Taranaki region shown in Figure
481 3, starting near the NPL substation and going south along the coast towards Wellington (at
482 the bottom of the North Island). In August 2018 the increases nearest NPL are red ETHD
483 circles (i.e., >0.3% ETHD increase), generally decreasing to orange (0.1-0.3% increase) and
484 then blue circles (0-0.1% increase), fairly steadily with distance from NPL. Importantly, there
485 are ETHD increases seen in all of the substations along this transmission line. A map of the
486 transmission lines and substations near NPL (and HWB and ROB) is shown in Figure 4. This
487 figure also displays whether the substations include transformers which are earthed (or not)
488 on the high voltage side (filled in red circles in Figure 4). Such earthing allows GIC to flow
489 into the transformer windings, potentially producing core saturation and hence harmonic
490 distortion. The other transformers (unfilled red circles in Figure 4) are not earthed on the high
491 voltage side (66 kV or above), but only on the low-voltage local supply side. Further
492 discussion on the earthing of New Zealand transformers in a GIC context can be found in
493 *Divett et al.* [2018] and *Mac Manus et al.* [2022a].

494

495 The upper left panel of Figure 4 shows the substations with earthed (red filled in) and non-
496 earthed transformers (red unfilled) going from New Plymouth (NPL) southwards towards
497 Bunnythorpe (BPE). To avoid clutter, only the substations for which we have ETHD data

498 along the NPL to BPE transmission line are labeled, as we will use these locations to analyze
499 ETHD propagation along a power line. Recall that GIC will only flow into transformer cores
500 for earthed substations, with examples being NPL, SFD, and BPE in this panel. As no GIC
501 will flow into the cores of transformers at HWA, WVY, BRK, WGN, and MTN, the cores
502 should not saturate, and thus no local harmonic production is expected. We conclude that the
503 ETHD increases seen in the non-earthed substations have propagated down the transmission
504 line from elsewhere; the most likely source is the NPL substation, as this substation included
505 a set of earthed single phase transformers, and the region showed large GMD-linked ETHD
506 increases maximized on NPL during its period of operation, which stopped once NPL was
507 decommissioned.

508

509 The lower panel of Figure 4 is a similar map for the lower South Island, another region
510 where clear GMD-linked ETHD increases were observed, and large changes after the
511 removal of a single phase transformer bank (in this case HWB T4). Once again, in
512 contrasting Figure 3 and the lower panel of Figure 4 we see evidence of ETHD increases in
513 substations without earthed transformers (e.g., BAL, BDE, and EDN), as well as a large
514 decrease in ETHD response after HWB T4 was decommissioned. This is, again, consistent
515 with ETHD propagating in the transmission network.

516

517 The upper right panel of Figure 4 shows the transmission lines and grounding status for the
518 West Coast region of the South Island, focused on Robertson Street (ROB) substation. Once
519 again, there is evidence of propagating ETHD, potentially starting at ROB and seen at the
520 non-earthed substations RFN and ATU. Uniquely, however, no transformers in the Robertson
521 Street substation are earthed such that GIC can enter cores and cause local saturation. This
522 apparent puzzle is addressed in Section 6.1.

523

524 **4.2 Further examination of GMD-linked ETHD propagation**

525 As noted earlier, there is evidence of GMD-produced ETHD increases propagating down
526 transmission lines, with decaying amplitudes along the line. We now investigate this in more
527 detail.

528

529 Figure 5 shows examples of the baseline corrected ETHD-increases along the transmission
530 line from NPL going southwards to MTN in the mid- and lower North Island (see Figure 4),
531 i.e., plotting the ETHD increases relative to distance along the transmission line from NPL.
532 Four examples from 3 GMD are shown. The red line is a linear fit of the decay with distance,
533 with the R^2 coefficient of determination given for each panel. As with the earlier maps in
534 Figure 3, subplots are shown in each panel showing the time series of the magnetic field
535 changes ($|H'|$, blue line), along with red lines marking the 10 min time window for this ETHD
536 decay plot. In this case we limit ourselves to a study of the transmission line from NPL to
537 MTN and do not include ETHD observations from BPE (Bunnythorpe). This is partly due to
538 the electrified train issue mentioned earlier, but also as we suspect some ETHD propagation
539 is occurring starting from the Wellington region, impacting BPE measurements. As can be
540 seen in Figure 5, the ETHD decays in an approximately linear fashion with distance along the
541 transmission line. We typically see quite good fits with quite high R^2 values. This is the
542 common situation for this substation, and indeed for most events at many of our substations
543 of interest (see section 4.3). We note that the fits are not perfect. For example in both
544 examples from August 2018 HWA is above the ETHD level seen in SFD, which is closer to
545 NPL. In contrast, in both April 2017 and September 2017 the observations from HWA fit
546 much closer to the linear relationship. In general the behavior is fairly consistent; every time
547 there is a significant ETHD response at NPL ($>0.05\%$ above baseline), it is found to decay in
548 a roughly linear fashion along the transmission line to BPE. However, the spread of ETHD is

549 likely to depend on the exact network state at that time, and hence will not be exactly the
550 same from event to event.

551

552 Figure 6 investigates ETHD decay patterns in the lower South Island. Before the removal of
553 HWB T4, strong ETHD increases are observed across the lower South Island, again with
554 evidence of a roughly linear decrease with transmission line distance from the source
555 substation. From October 2013 to September 2017 we see clear and approximately linear
556 decay rates of ETHD with distance measured from HWB, confirming the relationship seen
557 from NPL. After HWB T4 was decommissioned, the decay fits become weak or disappear.
558 An example is shown in Figure 6, for the GMD in November 2021. While there is a strong
559 ETHD increase observed at HWB, there is no evidence of propagation down the transmission
560 line.

561

562 Note that TWI often appears to have higher ETHD levels than predicted. This may be due to
563 TWI being a substation in which relatively high GIC are modelled [*Mac Manus et al.*,
564 2022b]; another possibility is the aluminum smelter at TWI serviced by that substation. The
565 smelter relies on specialist power transformers which have integrated power electronics
566 rectifiers to produce the high DC currents needed for smelting. An alternative explanation is
567 these systems are responding differently during GMD impacts.

568

569 Figures 5 and 6 showed evidence of GMD-linked ETHD increases propagating from NPL
570 and HWB. In Figure 7 we consider the situation on the West Coast of the South Island in the
571 same way, and investigate ETHD-increases around that substation. Of these, ROB substation
572 has the highest ETHD values so is assumed to be acting as a source, and we examine how the
573 ETHD values fall off with distance from ROB. As can be seen for the four examples of GMD
574 periods in Figure 7, it does seem that ROB is acting as a source, much as was earlier seen for

575 NPL and HWB. The R^2 coefficient of determination for the fitted decay with distance lines
576 are rather good quality, with values >0.8 and often >0.9 . Once again it appears as if ROB is
577 acting as a source of ETHD, despite the lack of GIC at those transformers. We discuss this
578 issue further in section 6.

579

580 **4.3 Summary: GMD-linked ETHD propagation**

581 We have examined all our GMD events and the specific substations of interest for evidence
582 of well-behaved ETHD propagation. Our criteria was a linear fit to the decay with distance
583 with $R^2 \geq 0.7$ and a source ETHD $\geq 0.05\%$ above baseline, plus a visual inspection of the decay
584 which was convincing "by eye". The results of this examination are shown in Table 3. In this
585 case a "yes" means the 3 criteria listed above. "Unclear" indicated the numerical criteria are
586 met, but the visual inspection is not fully convincing. "No" indicates a lack of propagation
587 evidence from the suggested source substation into the surrounding substations. As can be
588 seen from Table 3 the clearest evidence of ETHD propagating away from a source substation
589 is for ROB on the West Coast. NPL in the Taranaki region was a clear ETHD source causing
590 propagating ETHD increases during GMD in almost all the disturbances considered until the
591 substation was decommissioned in December 2019 (the exception is the relatively small
592 GMD on 27-28 Feb 2019). In contrast the situation for HWB and HEN is less clear; while
593 both substations appear to have local GMD-linked ETHD increases (as described in Table 2),
594 they do not always clearly propagate away from the source substation. In the case of ISL
595 local GMD-linked ETHD increases are very common (as seen from Table 2), but it is rare to
596 have clear examples of ETHD increases that appear to be sourced from this substation.

597

598 **4.4 Examining ETHD propagation with distance**

599 We now investigate the quality of the linear decay for propagating ETHD periods against
600 the magnitude of the ETHD produced at the suspected source substation. Here we include

601 events from all GMD where propagating ETHD is observed (noted by a "yes" in Table 3), for
602 all the substations of interest. This is shown in the upper panel of Figure 8. This panel shows
603 the relationship between the coefficient of determination (R^2), and the source ETHD
604 percentage level. We see that for low values of source ETHD there is a wider range of R^2
605 values, but the average R^2 value becomes less variable as the ETHD magnitude increases (i.e.,
606 in larger GMD).

607

608 The middle panel of Figure 8 examines how the propagating ETHD magnitudes decay
609 relative to the ETHD at the source substation, comparing all five selected substations. Here
610 we examine the fitted linear decay rates of ETHD for each source substation (i.e., ETHD
611 percentage per km along the transmission line) including multiple 10 min periods across all GMD
612 where clearly propagating ETHD was observed. The fitted linear decay rates are compared with
613 the ETHD found at the source substation. To create this panel we used all of the linear decay fits
614 which had $R^2 \geq 0.7$, a y-intercept $\text{ETHD} \geq 0.05\%$, and a reasonable number of data points. We plot
615 the y-intercepts of the decay fits, which are representative of the source ETHD (in %) at the
616 substation of interest, on the x-axis of the panel, and the slopes of the decay fits on the y-axis.
617 The steeper the lines shown on this panel, the faster the ETHD decays with distance along a
618 transmission line for a certain level of ETHD at the source. This panel shows that the
619 relationship for most source substations, especially for HWB, NPL, and ROB which have the
620 most periods with good quality propagation activity, have a very consistent linear relationship
621 between the ETHD at the source and the ETHD decay rate with distance. The R^2 value for
622 linear fits for those points is ≥ 0.94 . It seems reasonable these relationships could be extended to
623 describe larger GMD when larger source ETHD increases would be expected. The ISL and HEN
624 lines on this panel are limited to six and seven data points respectively, however these thirteen
625 data points are entirely consistent with the lines for other sub- stations, suggesting they would
626 follow a similar pattern if extended to a larger GMD.

627

628 Data points on the yellow line representing ROB as a source fall consistently below the
629 substations of interest, having a steeper slope of -0.00505 km^{-1} , compared to an average slope
630 of the other four substations of -0.0043 km^{-1} . This means that ETHD increases, even if they
631 were the same magnitude at the source, do not propagate as far from ROB as they do from
632 the other substations. One possibility is that this is caused by ETHD changes at ROB being
633 generated in a different way, as discussed later. However, the consistency of the ETHD fall-
634 off on propagation from the other earthed substations suggest the decay rate of -0.0043 km^{-1}
635 could be used to model such propagation during future, possible larger, events. Given the
636 substations of interest are for very different locations it also seems reasonable that the
637 observed decay rate could hold for all New Zealand substations. For example, the observed
638 decay rates do not depend on whether the substation is connected by 110 or 220 kV
639 transmission lines (as shown in the middle panel of Figure 8).

640

641 **5. Correlation with transformers modeled to have high GIC**

642 **5.1 Comparison with GIC modeling**

643 As briefly mentioned in the introduction *Mac Manus et al.* [2022b] recently used the New
644 Zealand validated GIC model to investigate GIC hazard levels for a "Carrington class" GMD,
645 based on the UK government "Reasonable Worst-Case Scenario" for a GMD [*Hapgood et al.*,
646 2021]. The *Mac Manus et al.* [2022b] study found the at-risk transformers were not localized
647 to any specific region of New Zealand but extended across all regions and include most of the
648 major population centers. Figure 10 of that study summarizes the locations of substations
649 with the highest GIC magnitudes.

650

651 ETHD increases provide an independent way of confirming the GIC magnitude modeling
652 described above. Some locations, particularly in the North Island, had no GIC monitoring
653 data when the modeling was undertaken; such that the modeling relied on the network
654 topology information from Transpower and GIC observations mostly from the lower and mid
655 South Island (see the description in *Mac Manus et al.* [2022a]). High currents are predicted in
656 the HWB and ISL substations, and confirmed through GMD-linked ETHD increases but this
657 modeling was strongly informed by GIC observations in those substations. However,
658 modeling also predicted high currents should be present in the NPL substation [*Mukhtar et*
659 *al.*, 2020], as well as the HEN substation [*Mac Manus et al.*, 2022b], where no GIC
660 measurements existed. The modeling results are consistent with the GMD-linked ETHD
661 increases reported in the current study, providing additional confidence in the GIC modeling.

662

663 5.2 Single phase versus three phase transformers and ETHD

664 The dramatic changes in GMD-linked ETHD occurrence when single phase units were
665 removed (HWB and NPL) demonstrates the higher sensitivity of single phase transformers to
666 GIC leading to ETHD production. When considering GIC danger levels using industry
667 provided GIC thresholds of current magnitude and time, *Mac Manus et al.* [2022b] reported
668 that thermal impacts would occur at much lower levels for a single phase transformer than a
669 three-phase transformer. Clearly, the ETHD occurrence in the New Zealand network
670 becomes much lower once the single phase units are removed, with remaining increases
671 likely linked to single phase units in ISL and HEN. However, we note that ETHD increases
672 do not stop in the HWB substation after the decommissioning of HWB T4, as seen in Figures
673 2 and 3, and Table 2. After HWB T4 is removed the remaining earthed transformers are three
674 phase design, with lower sensitivity to GIC. However, currents in the remaining transformers
675 in HWB and SDN are still large, with HWB T6 and SDN T2 having roughly the same peak
676 GIC magnitudes as HWB T4 experienced (see for example, Figure 3 of *Mac Manus et al.*

677 [2022a] or Table S9 from that paper). Continued GMD-linked ETHD increases observed at
678 HWB, after the single phase transformers had been removed, indicates that the remaining
679 three phase units were still being driven into partial saturation by the very large GIC
680 magnitudes in the Dunedin substations. The lower panel of Figure 8 shows how GMD-linked
681 ETHD increases depended on GIC magnitude before and after the HWB T4 unit was
682 decommissioned in late November 2017. As expected, there is a marked decrease in ETHD
683 after the single-phase unit is taken out of service. The same GIC magnitude observed in the
684 main HWB transformers (HWB T4 beforehand, HWB T6 afterwards) produces one-third the
685 ETHD change once the single phase transformer is decommissioned, consistent with the
686 findings in *Clilverd et al.* [2020] using VLF observations.

687 **6. Discussion**

688

689 **6.1 ETHD production from Roberson Street (ROB) substation**

690 As noted above, the Robertson Street (ROB) substation appears to act as a source of GMD-
691 linked ETHD, despite there being no earthed transformers present in this substation (either
692 single phase or three phase units). As well as checking this with Transpower New Zealand
693 Ltd, the grid operator, we also communicated with the local owner of this substation, who
694 confirmed the details we held (private communicate, Dale Ross, network manager, Buller
695 Electricity Ltd). As such, we have no evidence that GIC could be saturating transformers at
696 this substation to produce the clearly observed harmonics.

697

698 The GMD-linked ETHD appearing from ROB is most likely caused by a resonance
699 occurring in this substation, amplifying ETHD produced in some other substation, and
700 causing ROB to act like an ETHD source. For the following discussion we direct the
701 interested reader to the textbook *Arrillaga and Watson* [2003]. A real-world substation
702 includes a number of inductive and capacitive elements, which will have frequency

703 dependent responses. The combined system of such elements, for example in a substation,
704 produces a power system with a resonant frequency (also known as the "natural" or "critical"
705 frequency) dependant on the elements in the system. Such resonances can be identified by the
706 application of nodal admittance matrix analysis [e.g., *Huang et al.*, 2007; *Amornvipas and*
707 *Hofmann*, 2010; *Pană and Băloi*, 2014]. This analysis involves the generation of an N by N
708 Nodal Admittance matrix, where N is the number of busses in the system being analysed. In
709 this context, a bus (or bus bar), usually located within a substation, is essentially a connector
710 for multiple high voltage loads, and is fixed at a certain voltage. There can be multiple bus
711 bars within a substation, for example combinations of 66, 110, and 220 kV bus systems.
712 Admittance is defined as the inverse of impedance, measured in Siemens. A higher
713 admittance means it is easier for current to flow; admittance is more applicable to AC power
714 systems than resistance as it takes into account other dynamic factors, such as reactance
715 [*Grainger and Stevenson*, 1994]. Nodal admittance matrix harmonic modelling allows one to
716 identify resonant frequencies in a network. It is possible for the resonant frequency to overlap
717 with the system operational frequency (or that of its harmonics), which then leads to power
718 quality issues and can negatively impact equipment in the substation [e.g., *Lemieux*, 1990;
719 *Eghedarpour et al.*, 2014].

720

721 The New Zealand Electricity Authority provides detailed data on the New Zealand electrical
722 network to allow transmission engineers and technical analysts to undertake power systems
723 analysis [*Electricity Authority*, 2023]. These data were originally sourced from Transpower
724 New Zealand Ltd, the system operator and are designed to be used by the DIgSILENT
725 Powerfactory power system analysis software application. We have used Powerfactory to
726 undertake Harmonic Modelling focused on the Robertson Street Substation, allowing
727 resonances to be identified. The simulation process consisted of running a frequency sweep
728 up to the 10th harmonic (500 Hz) and analyzing the impedance-frequency characteristic of

729 the busbars connected to transmission lines going south-west and north-east of ROB
730 substation. In a power system there are two different types of resonances; series and parallel.
731 Series resonances at a specific bus bar are indicated by the admittance for the node sharply
732 increasing around a certain frequency and the admittance sharply decreasing around a certain
733 frequency for parallel resonance. Series resonances create current distortion and parallel
734 resonances create voltage distortion. In the modelling loads were switched out of the
735 simulation system to see their affect on the impedance frequency characteristic, and hence
736 identify the combination of elements leading to the resonance. This analysis identified that
737 the 33 kV busbar in the ROB substation has multiple parallel and series resonances around
738 the 6th harmonic, providing a potential explanation for the GMD-linked ETHD appearing to
739 come from ROB. As our measurements are of voltage ETHD, and show evidence of
740 propagating harmonics, we conclude this is most likely due to parallel resonances leading to
741 6th order voltage harmonics.

742

743 One remaining question is the source of the ETHD which is apparently amplified by a
744 resonance at the ROB substation. The best candidate which could be potential sources of the
745 original ETHD is from the Kikiwa (KIK) earthed substation, shown to the east of ROB in
746 Figure 4 (top right panel), ~100 km from ROB. Naively the best candidate might be thought
747 to be the single phase unit at KIK (KIK T1). However, it is more likely that the source is the
748 three phase unit at KIK (KIK T2), as modeling has shown it to be a transformer in the top ten
749 list for GIC magnitudes for New Zealand [*Mac Manus et al.*, Table 2, 2022b], with GIC
750 magnitudes ~4 times higher than KIK T1. This is caused by the series winding resistances of
751 KIK T2 being ~4 times smaller than KIK T1. KIK is not a large source for ETHD, but the
752 observations indicate it has observable ETHD-levels during GMD, although lower than seen
753 at ROB. For example, during the August 2018 GMD the KIK substation showed voltage
754 ETHD peaks which were roughly one-third of the magnitude of those at ROB. There is

755 additional evidence to support KIK as a potential ETHD source; while there is a fairly clear
756 and consistent drop-off in ETHD magnitudes going "south" from ROB towards HKK (as
757 seen in the upper right panel of Figure 4); this is not true going "east" of ROB towards KIK,
758 potentially indicating that the combination of ROB and KIK interferes with the propagation
759 pattern. Thus we conclude harmonic disturbances generated at the KIK substation resonate
760 and are amplified at the 33 kV busbar in the ROB substation, producing the observed
761 signature.

762

763 Note that we do not claim that this modeling does conclusively demonstrate that the
764 apparent ROB source is a resonance, or that the original GMD-produced is from KIK T2. The
765 New Zealand power system network detailed data has not been verified for use in harmonic
766 studies at this point. The modeling provides a good indicator of likely harmonic resonances, but
767 field work would be required to test the modeling and these conclusions. Such additional work
768 is beyond the scope of the current study, but is under consideration for the future.

769

770 **6.2 ETHD increases in Henderson**

771 The earlier work by *Rodger et al.* [2020] stimulated much interest by our industry partner,
772 Transpower New Zealand. Previous to that research it was widely believed by the
773 Transpower staff that the GIC hazard was confined to the lower South Island. Evidence that
774 GMD-linked stressed transformers existed in the upper South Island and Taranaki region
775 caused a major rethink and new appreciation of the space weather hazard. Early results from
776 the extreme GMD modeling which identified the Henderson (HEN) substation in Auckland
777 city as having high GIC also helped to break previous misconceptions (that work was
778 eventually published as *Mac Manus et al.* [2022b]). The research reported here confirms
779 GMD-linked ETHD increases in HEN, indicating transformers in New Zealand's largest city

780 likely has a significant space weather risk. The *Mac Manus et al.* [2022b] GIC modeling and
781 current ETHD analysis caused Transpower to install DC measuring instruments in the HEN
782 substation. Recent G4-level geomagnetic storms have confirmed the occurrence of significant
783 GIC at HEN, roughly one-quarter of that seen in Dunedin.

784

785 Evidence of significant GIC and ETHD increases (i.e., stressed transformers) in HEN
786 suggests the space weather risk can extend significant distances equatorwards, even in a small
787 country with relatively short power lines (when compared with Australia or South Africa, for
788 example). We assume that global locations within these geomagnetic latitude ranges might
789 possibly have high enough GIC to produce transformer saturation and harmonic production,
790 i.e., what occurs in New Zealand might happen elsewhere on Earth. Using the International
791 Geomagnetic Reference Field (IGRF), 13th Generation, revised in 2020 [*Alken et al.*, 2021]
792 we have found equivalent locations to HEN elsewhere on Earth to provide wider global
793 context using the online geomagnetic coordinate calculator provided by the British
794 Geological Survey
795 (http://www.geomag.bgs.ac.uk/data_service/models_compass/coord_calc.html). The
796 Henderson substation is located at 36.88° S, 174.63° E in geographic coordinates, which for
797 epoch 2017 has a quasi-dipole latitude = -42.66° and a quasi-dipole longitude = 256.62°
798 ($L=1.85$). For Europe this is geomagnetically essentially equivalent to the city of Budapest
799 (geographic: 47.50° N, 19.04° E, geomagnetic quasi-dipole: 42.64°, 93.54°), for North
800 America both San Francisco, California (geographic: 37.78° N, 122.42° W, geomagnetic
801 quasi-dipole: 42.82°, 302.63°), and Charleston, South Carolina (geographic: 32.78° N,
802 79.93° W, geomagnetic quasi-dipole: 42.28°, 355.79°), and for Asia the Russian city of
803 Khabarovsk (geographic: 48.48° N, 135.07° E, geomagnetic quasi-dipole: 42.38°, 208.58°).

804

805 **7. Summary**

806 Space weather can adversely affect electrical power infrastructure through the generation of
807 GIC and the production of harmonic distortion to the AC waveform generated by half-cycle
808 saturation of transformers. Half-cycle saturation of transformers leads to even order
809 harmonics, and thus investigating Even Total Harmonic Distortion (ETHD) during GMD can
810 provide insights into the impact of space weather on an electrical network.

811

812 This is the second study to investigate ETHD occurrence in the New Zealand electrical
813 network. Here we build on the earlier work [*Rodger et al.*, 2020], which primarily focused on
814 a single GMD. We expand that work to analysis ETHD changes across 10 GMD occurring
815 from late 2013 to 2023, looking at ETHD changes monitored at 139 locations across the New
816 Zealand power network. During that time some significant changes occurred in the power
817 network, at locations known to be impacted by space weather: the removal of the Halfway
818 Bush (HWB) single phase transformer T4 in November 2017, and the decommissioning of
819 the New Plymouth (NPL) substation in December 2019. NPL also contained an earthed
820 single phase transformer. Following the decommissioning of those assets there were dramatic
821 changes in GMD-linked ETHD increases at the HWB substation and also in substations
822 which are within 150-200 km from both HWB and NPL substations. ETHD levels during
823 GMD substantially decrease across the region after the equipment removal. We have
824 identified 5 substations which appear to act as sources for GMD-linked ETHD, 4 of which
825 are consistent with half cycle saturation by GIC at single phase units, which then propagates
826 into the surrounding network. The nature of the propagation is consistent (i.e., roughly the
827 same ETHD decay with distance), which should allow future studies to model the
828 propagation of ETHD across the power network in future events.

829

830 The analysis undertaken in the current study also shows that ETHD observations are not as
831 simple and direct as was earlier concluded by *Rodger et al.* [2020]. Some ETHD increases
832 appear to occur outside of GMD, and are likely due to unbalanced loads due to poorly
833 installed industrial equipment or electrical train drive systems. During GMD periods we also
834 show evidence of a ETHD source substation which cannot be explained by locally stressed
835 transformers at Robertson Street (ROB) on the West Coast of the South Island. It appears
836 most likely this is due to resonances occurring inside this substation, due to ETHD increases
837 produced elsewhere,

838

839 Previous modeling studies have identified transformers in substations which are predicted to
840 experience high-GIC during significant GMD. Some of these were locations for which GIC-
841 observations had already identified this, but some were not. Examples of the latter are NPL
842 and HEN, where we find significant ETHD sources, consistent with transformers stressed by
843 GIC. The ETHD analysis in the current study helps independently confirm the extreme storm
844 modeling of *Mac Manus et al.* [2022b]. We have also shown evidence of stressed
845 transformers sited in quite an equatorward location (HEN in Auckland), equivalent to
846 Budapest or San Francisco in the Northern Hemisphere.

847

848 **Acknowledgments.** This research was supported by the New Zealand Ministry of
849 Business, Innovation & Employment Hazards and Infrastructure Research Fund Contract
850 UOOX2002. The authors would like to thank Transpower New Zealand for supporting this
851 study.

852

853 **Open Research.** Eyrewell magnetometer data availability is described at:
854 <https://intermagnet.org/metadata/#/> (select EYR) and
855 https://intermagnet.org/new_data_download.html. . The New Zealand LEM DC and

856 harmonic distortion data were provided to us by Transpower New Zealand with caveats and
857 restrictions. This includes requirements of permission before all publications and
858 presentations. In addition, we are unable to directly provide the New Zealand LEM DC
859 data, derived GIC observations, or the harmonic distortion data. Requests for access to the
860 measurements need to be made to Transpower New Zealand. At this time the contact point
861 is Michael Dalzell (Michael.Dalzell@transpower.co.nz). We are very grateful for the
862 substantial data access they have provided, noting this can be a challenge in the Space
863 Weather field [*Hapgood and Knipp, 2016*].

864

865 **References**

- 866 Alken, P., E. Thébault, C. D., Beggan, H. Amit, J. Aubert, J. Baerenzung, T. N. Bondar, W. J.
867 Brown, S. Califf, et al. (2021). International Geomagnetic Reference Field: the thirteenth
868 generation, *Earth Planets Space* 73, 49. <https://doi.org/10.1186/s40623-020-01288-x>
869 Amornvipas, C., and L. Hofmann (2010), Resonance analyses in transmission systems:
870 Experience in Germany, Proc. IEEE PES Gen. Meeting, doi: 10.1109/PES.2010.5588098.
871 Arrillaga, J. and, N. R. Watson (2003), *Power System Harmonics*, 2nd Edition, Wiley, ISBN:
872 978-0-470-85129-6 October 2003.
- 873 Baker, D. N., et al. (2008), *Severe Space Weather Events: Understanding Societal and*
874 *Economic Impacts*, 144 pp., National Academies Press, Washington, D. C., USA
- 875 Béland, J., and K. Small (2004), Space weather effects on power transmission systems: The
876 cases of Hydro-Québec and Transpower New Zealand Ltd, in *Effects of Space Weather on*
877 *Technological Infrastructure*, edited by I. A. Daglis, pp. 287–299, Kluwer Acad.,
878 Netherlands.
- 879 Boteler, D. H. (2015). The Impact of Space Weather on the Electric Power Grid. In
880 *Heliophysics V. Space Weather and Society*, by C. J. Schrijver, F. Bagenal, and Sojka.
881 Palo Alto, CA: Lockheed Martin Solar & Astrophysics Laboratory
- 882 Boteler, D.H., Shier, R.M., Watanabe, T. and Horita, R.E. (1989). Effects of geomagnetically
883 induced currents in the BC Hydro 500 kV system, *IEEE Trans. Power Delivery*, 4, 818-
884 823.

- 885 Clilverd, M. A., Rodger, C. J., Brundell, J. B., Dalzell, M., Martin, I., Mac Manus, D. H., et
886 al. (2018). Long-lasting geomagnetically induced currents and harmonic distortion
887 observed in New Zealand during the 7–8 September 2017 disturbed period. *Space*
888 *Weather*, 16, 704–717. <https://doi.org/10.1029/2018SW001822>
- 889 Clilverd, M. A., Rodger, C. J., Brundell, J. B., Dalzell, M., Martin, I., Mac Manus, D. H., &
890 Thomson, N. R. (2020). Geomagnetically induced currents and harmonic distortion: High
891 time resolution case studies. *Space Weather*, 18, e2020SW002594.
892 <https://doi.org/10.1029/2020SW002594>
- 893 Divett, T., G. S. Richardson, C. D. Beggan, C. J. Rodger, D. H. Boteler, and M. Ingham
894 (2018), Transformer-level modeling of Geomagnetically Induced Currents in New
895 Zealand's South Island, *Space Weather*, 16, 718–735, doi:
896 <http://dx.doi.org/10.1029/2018SW001814>.
- 897 Divett, T., M. Ingham, C. D. Beggan, G. S. Richardson, C. J. Rodger, A. W. P. Thom-
898 son, and M. Dalzell (2017), Modeling Geoelectric Fields and Geomagnetically Induced
899 Currents Around New Zealand to Explore GIC in the South Island's Electrical Trans-
900 mission Network, *Space Weather*, 15(10), 1396–1412, doi:10.1002/2017SW001697.
- 901 Divett, T., Mac Manus, D. H., Richardson, G. S., Beggan, C. D., Rodger, C. J., & Ingham,
902 M., et al. (2020). Geomagnetically induced current model validation from New Zealand's
903 South Island. *Space Weather*, 18, e2020SW002494.
904 <https://doi.org/10.1029/2020SW002494>.
- 905 Dong, X., Y. Liu, and J. G. Kappenman (2001), Comparative analysis of exciting current
906 harmonics and reactive power consumption from GIC saturated transformers, 2001 IEEE
907 Power Engineering Society Winter Meeting. Conference Proceedings, doi:
908 10.1109/PESW.2001.917055, 2001.
- 909 Eghtedarpour, N., M. A. Karimi, and M. Tavakoli (2014), Harmonic resonance in power
910 systems - a documented case, Proc. 16th Int. Confe. on Harmonics and Quality of Power,
911 doi: 10.1109/ICHQP.2014.6842806, 2014.
- 912 Electric Power Research Institute (EPRI) (1983), Mitigation of geomagnetically induced and
913 dc stray currents, EPRI, Palo Alto, CA: Report EL-3295.
- 914 Electric Power Research Institute (EPRI). 2014. Analysis of Geomagnetic Disturbance
915 (GMD) Related Harmonics, Technical Update 3002002985. 2014. Available online:
916 <https://www.epri.com/research/products/000000003002002985> (accessed on 22
917 September 2023).

- 918 Electricity Authority, Electricity Market Information website,
919 <https://www.emi.ea.govt.nz/Wholesale/Datasets/Transmission/PowerSystemAnalysis/PowerFactoryCaseFiles> (accessed on 2 November 2023).
- 921 Grainger, J. J., and W. D. Stevenson, (1994), *Power System Analysis*, McGraw-Hill.
- 922 Guillon, S., Toner, P., Gibson, L., and Boteler, D. (2016). A Colorful Blackout: The Havoc
923 Caused by Auroral Electrojet Generated Magnetic Field Variations in 1989. *IEEE Power
924 & Energy Magazine*, 14(6).
- 925 Hapgood, M., and D. J. Knipp (2016), Data Citation and Availability: Striking a Balance
926 Between the Ideal and the Practical, *Space Weather*, 14, 919–920,
927 doi:10.1002/2016SW001553.
- 928 Hapgood, M., Angling, M. J., Attrill, G., Bisi, M., Cannon, P. S., Dyer, C., et al. (2021).
929 Development of space weather reasonable worst-case scenarios for the UK National Risk
930 Assessment. *Space Weather*, 19, e2020SW002593,
931 <https://doi.org/10.1029/2020SW002593>.
- 932 Huang, Z., Y. Cui, and W. Xu (2007), Application of Modal Sensitivity for Power System
933 Harmonic Resonance Analysis, *IEEE Trans. Power Sys.*, 22(1),
934 doi:10.1109/TPWRS.2006.883678.
- 935 Ingham, M., C. J. Rodger, T. Divett, M. Dalzell, and T. Petersen, Assessment of GIC based
936 on transfer function analysis, *Space Weather*, 15, doi:10.1002/2017SW001707, 5, 1615–
937 1627, 2017.
- 938 JASON (2011), Impacts of Severe Space Weather on the Electric Grid (JSR-11-320), The
939 MITRE Corporation, McLean, Virginia, USA.
- 940 Lemieux, G. (1990), Power system harmonic resonance-a documented case, *IEEE Trans. Ind.
941 App.*, 26(3), 483 - 488, doi: 10.1109/28.55959.
- 942 Mac Manus, D. H., C. J. Rodger, A. Renton, J. Ronald, D. Harper, C. Taylor, M. Dalzell, T.
943 Divett, and M. A. Clilverd (2023), Geomagnetically Induced Current Mitigation in New
944 Zealand: Operational Mitigation method development with Industry input, *Space Weather*,
945 21, e2023SW003533, doi:10.1029/2023SW003533.
- 946 Pană, A., and Băloi, A. (2014). Identify Resonant Frequencies in AC Distribution Networks
947 A Numerical Example Part I - Harmonic Nodal Admittance Matrix Method. *Procedia -
948 Social and Behavioural Sciences*, 191, 1225-1232, doi:10.1016/j.sbspro.2015.04.369.
- 949 Mac Manus, D. H. (2023). Geomagnetically Induced Currents: Validating Observations and
950 Modelling in New Zealand (Thesis, Doctor of Philosophy). University of Otago. Retrieved
951 from <http://hdl.handle.net/10523/15443>.

- 952 Mac Manus, D. H., Rodger, C. J., Dalzell, M., Renton, A., Richardson, G. S., Petersen, T., &
953 Clilverd, M. A. (2022b). Geomagnetically induced current modeling in New Zealand:
954 Extreme storm analysis using multiple disturbance scenarios and industry provided hazard
955 magnitudes. *Space Weather*, 20, e2022SW003320.
956 <https://doi.org/10.1029/2022SW003320>.
- 957 Mac Manus, D. H., Rodger, C. J., Ingham, M., Clilverd, M. A., Dalzell, M., Divett, T., et al.
958 (2022). Geomagnetically induced current model in New Zealand across multiple
959 disturbances: Validation and extension to non-monitored transformers. *Space Weather*, 20,
960 e2021SW002955. <https://doi.org/10.1029/2021SW002955>.
- 961 Marshall, R. A., M. Dalzell, C. L. Waters, P. Goldthorpe, and E. A. Smith (2012),
962 Geomagnetically induced currents in the New Zealand power network, *Space Weather*, 10,
963 S08003, doi:10.1029/2012SW000806.
- 964 Mukhtar, K., Ingham, M., Rodger, C. J., Mac Manus, D. H., Divett, T., Heise, W., et al.
965 (2020). Calculation of GIC in the North Island of New Zealand using MT data and thin-
966 sheet modeling. *Space Weather*, 18, e2020SW002580.
967 <https://doi.org/10.1029/2020SW002580>
- 968 NERC. (2013). Network applicability project 2013-03. EOP-010-1. NERC.
969 North American Electric Reliability Corporation (NERC). 2013. Network Applicability
970 Project 2013, 03 (geomagnetic disturbance mitigation) EOP-010-1 (geomagnetic
971 disturbance operations). Available online:
972 https://www.nerc.com/pa/Stand/Project201303GeomagneticDisturbanceMitigation/ApplicableNetwork_clean.pdf (accessed on 22 September 2023).
- 974 Oughton, E. J., A. Skelton, R. B. Horne, A. W. P. Thomson, and C. T. Gaunt (2017),
975 Quantifying the daily economic impact of extreme space weather due to failure in
976 electricity transmission infrastructure, *Space Weather*, 15, doi:10.1002/2016SW001491.
- 977 Piccinelli, R., and E. Krausmann (2015), Space weather impact on the Scandinavian
978 Interconnected Power transmission System, EUR 27571EN, IBN 978-92-79-537615,
979 doi:10.2788/939973.
- 980 Rodger, C. J., Clilverd, M. A., Mac Manus, D. H., Martin, I., Dalzell, M., Brundell, J. B., et
981 al. (2020). Geomagnetically Induced Currents and Harmonic Distortion: Storm-time
982 Observations from New Zealand. *Space Weather*, 18, e2019SW002387.
983 <https://doi.org/10.1029/2019SW002387>.

984 Rodger, C. J., et al. (2017). Long-term geomagnetically induced current observations from
985 New Zealand: Peak current estimates for extreme geomagnetic storms. *Space Weather*, 15,
986 1447–1460. <https://doi.org/10.1002/2017SW001691>.

987 Samuelsson, O. (2013). *Geomagnetic Disturbances and Their Impact on Power Systems -*
988 *Status Report 2013*. Sweden: Lund University.

989 Transpower (2021), 2021 Integrated Transmission Plan Narrative, Transpower New Zealand
990 Ltd., Wellington, available online from:
991 https://static.transpower.co.nz/public/uncontrolled_docs/ITP%20Narrative%202021.pdf.

992 United Nations Committee on the Peaceful Uses of Outer Space Expert Group on Space
993 Weather (2017), Report on Thematic Priority 4: International Framework for Space
994 Weather Services for UNISPACE+50 (A/AC.105/1171). Available online from:
995 www.unoosa.org/oosa/oosadoc/data/documents/2018/aac.105/aac.1051171_0.html

996 Watson, N. R., and J. Arrillaga (2018), *Power Systems Electromagnetic Transients*
997 *Simulation*, 2nd Edition, The Institution of Engineering and Technology, ISBN: ISBN-13:
998 978-1-78561-499-6.

999 _____

1000 Malcolm Crack, Daniel H. Mac Manus, and Craig J. Rodger, Department of Physics,
1001 University of Otago, P.O. Box 56, Dunedin, New Zealand. (email:
1002 malcolmcrack12@gmail.com, daniel.macmanus@otago.ac.nz, craig.rodger@otago.ac.nz).

1003 Mark A. Clilverd, British Antarctic Survey (UKRI-NERC), High Cross, Madingley Road,
1004 Cambridge CB3 0ET, England, U.K. (e-mail: macl@bas.ac.uk).

1005 Michael Dalzell and Ian Martin, Transpower New Zealand Ltd., Waikoukou, 22 Boulcott
1006 Street, PO Box 1021, Wellington, New Zealand. (email: Michael.Dalzell@transpower.co.nz;
1007 Ian.Martin@ems.co.nz).

1008 Tanja Petersen, GNS Science, 1 Fairway Drive, Avalon, Lower Hutt 5011, New Zealand
1009 (email: T.Petersen@gns.cri.nz).

1010 Soren Subritzky and Neville Watson, 1Department of Electrical and Computer
1011 Engineering, University of Canterbury, 69 Creyke Road Christchurch, New Zealand (email:
1012 soren.subritzky@pg.canterbury.ac.nz, neville.watson@canterbury.ac.nz).

1013

12 March 2024 (NZST)

1014

1015 RODGER ET AL.: GMD-LINKED THD OBSERVATIONS FROM NEW ZEALAND

1016

1017 **TABLES**

1018

1019

GMD Time Period [UT]	Max. H' (nT/min) 1 min res.	Max. H' (nT/min) 10 min res.
2 Oct 2013	85.6	10.8
17-18 Mar 2015	68.4	7.7
22-24 April 2017	18.7	7.5
7-9 Sept 2017	33.3	12.0
26-27 Aug 2018	42.7	15.6
27-28 Feb 2019	7.7	4.4
12-13 Oct 2021	32.1	5.8
3-4 Nov 2021	31.6	16.2
23-24 Mar 2023	18.2	8.6
23-25 Apr 2023	40.1	10.9

1020

1021 **Table 1.** Geomagnetic disturbances (GMD) investigated in the current study. The maximum1022 rate of change of the horizontal component of the magnetic field (H') listed are based on

1023 observations from the Eyrewell (EYR) magnetic observatory, and are provided for 1- and 10-

1024 time resolution. The three largest GMD are highlighted in bold in this table, and also in Table

1025 2.

1026

1027

1028

GMD Time Period [UT]	HWB	NPL	ROB	ISL	HEN
2 Oct 2013	Yes	Yes	-	Yes	No
17-18 Mar 2015	Yes	Yes	Yes	Yes	Unclear
22-24 April 2017	Yes	Yes	-	Yes	Yes
7-9 Sept 2017	Yes	Yes	Yes	Yes	Yes
26-27 Aug 2018	Yes	Yes	Yes	Yes	Yes
27-28 Feb 2019	No	Yes	Yes	Yes	No
12-13 Oct 2021	Unclear	-	Yes	Yes	Yes
3-4 Nov 2021	Yes	-	Yes	Yes	Yes
23-24 Mar 2023	Yes	-	Yes	No	Yes
23-25 Apr 2023	No	-	Yes	No	Yes

1029

1030 **Table 2.** Geomagnetic disturbances (GMD) investigated in the current study indicating if a

1031 clear ETHD response is observed at the 5 key substations identified in Section 3. The

1032 substations are ordered from south to north, i.e., moving equatorwards in the Southern

1033 Hemisphere. A "-" in the table refers to missing data.

1034

1035

1036

1037

GMD Time Period [UT]	HWB	NPL	ROB	ISL	HEN
2 Oct 2013	Yes	Yes	Yes	No	No
17-18 Mar 2015	Yes	Yes	Yes	No	Unclear
22-24 April 2017	No	Yes	Unclear	No	No
7-9 Sept 2017	Yes	Yes	Yes	Yes	Yes
26-27 Aug 2018	Unclear	Yes	Yes	Unclear	Yes
27-28 Feb 2019	No	No	Yes	No	No
12-13 Oct 2021	No	No	Yes	No	No
3-4 Nov 2021	No	No	Yes	No	No
23-24 Mar 2023	No	No	Yes	No	No
23-25 Apr 2023	No	No	Unclear	No	No

1038

1039 **Table 3.** Geomagnetic disturbances (GMD) investigated in the current study indicating if a

1040 well-fit propagating ETHD response is observed, focusing on the 5 key substations. See text

1041 for details.

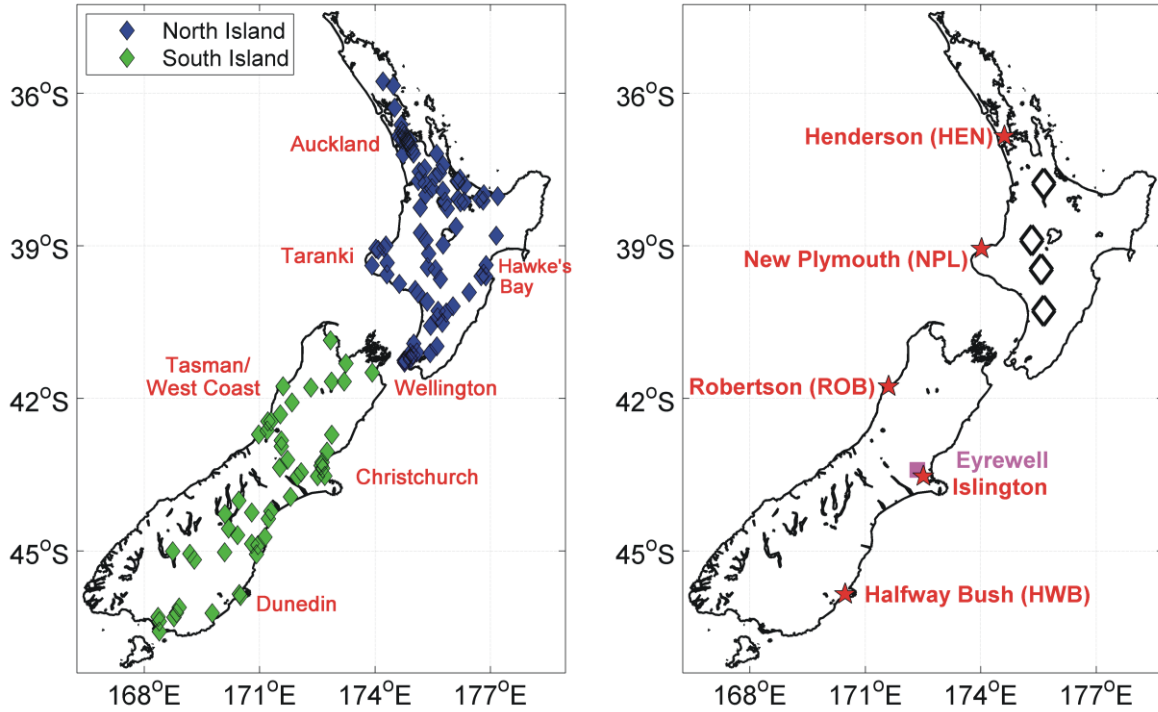
1042

1043

1044 **FIGURES**

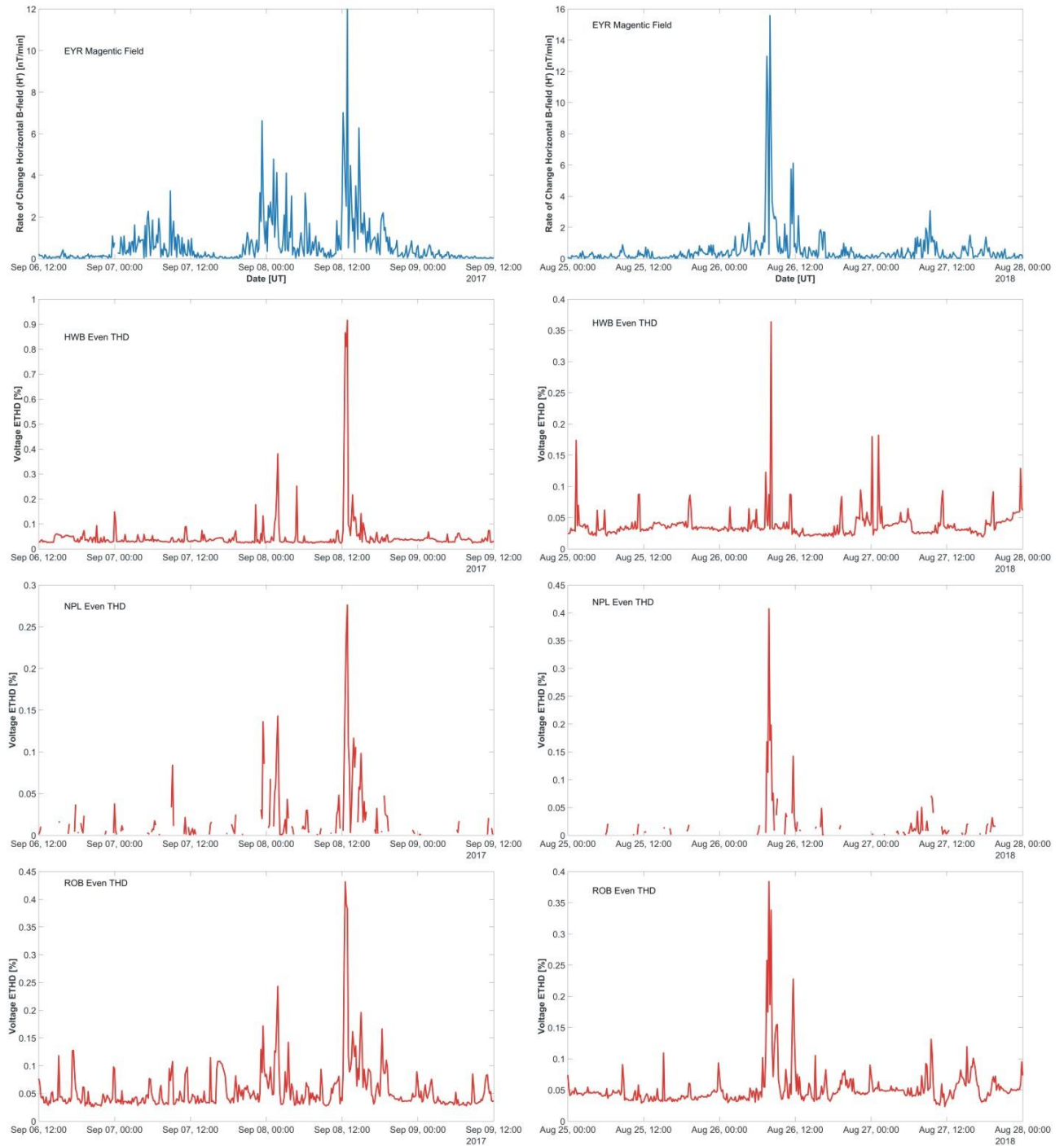
1045

1046



1047

1048 **Figure 1.** Left hand panel: Locations of the even-THD observations used in the current
 1049 study. A total of 139 substations provide even-THD measurements in the time period
 1050 considered (2013-2023), covering the entire Transpower electricity transmission network.
 1051 Right hand panel: map of locations of specific substations of interest discussed in the text
 1052 (red stars and white diamonds), as well as the Eyrewell magnetic observatory (magenta
 1053 square).



1054

1055

Figure 2. Time variation in the rate of change of the horizontal component of the EYR-

1056

observed magnetic field (upper row), and the variation in even order voltage THD measured

1057

at three different substations (lower three rows). The substations examined are HWB, NPL,

1058

and ROB. The left hand column is a GMD in September 2017, the right hand column is for

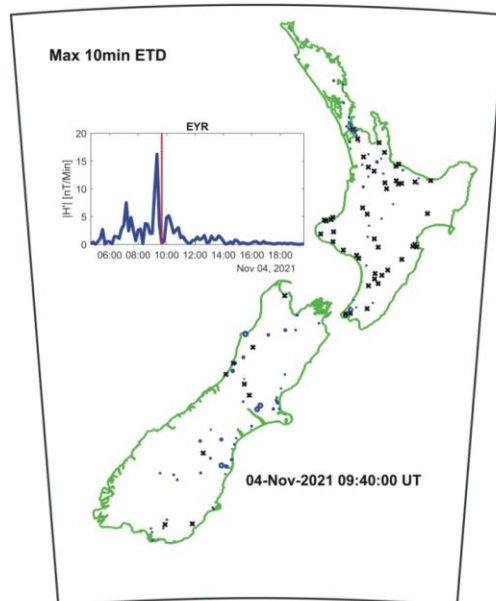
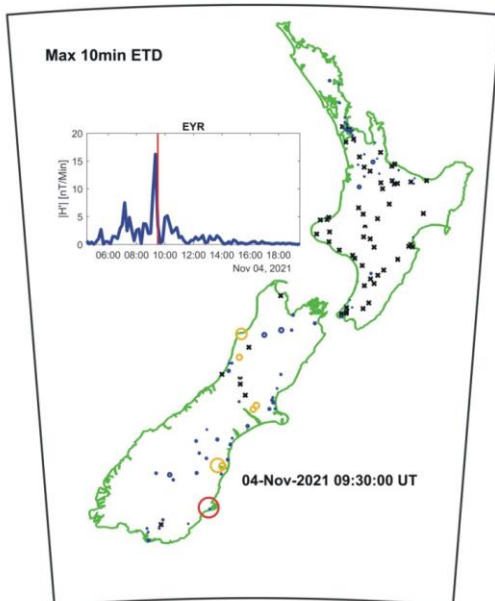
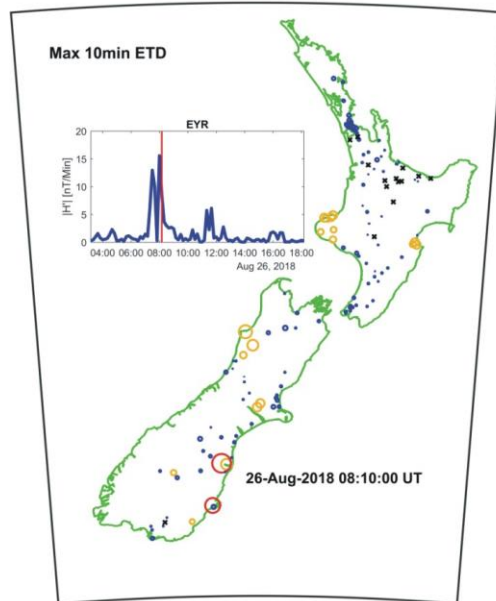
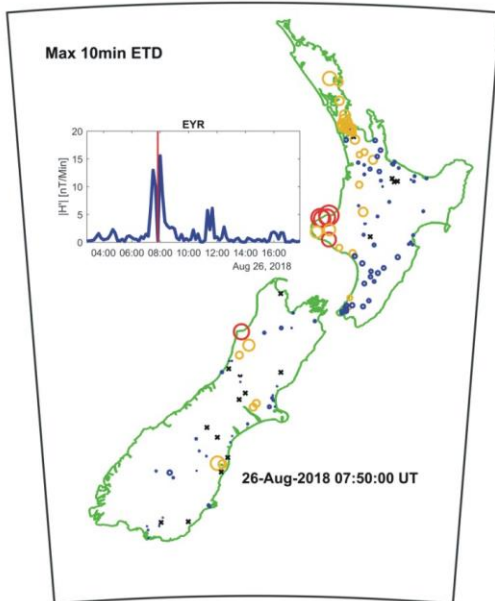
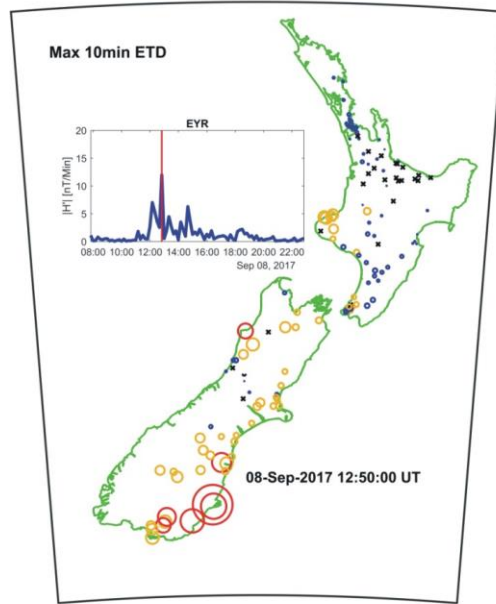
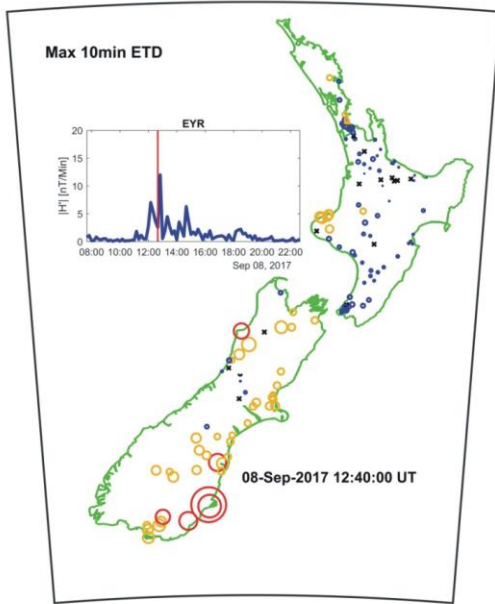
1059

August 2018. All data is shown with 10 min time resolution, the default for the THD

1060

observations.

1061

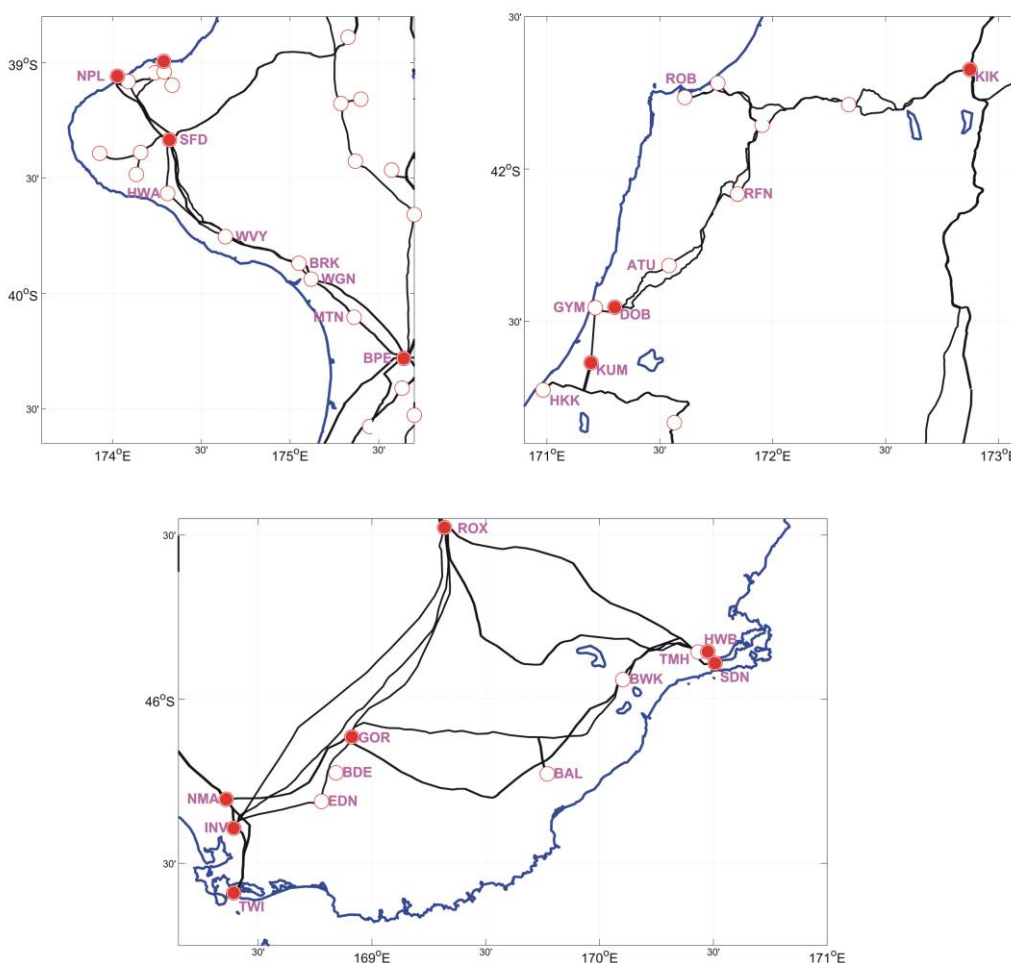


1063 **Figure 3.** Maps showing the variation in baseline corrected ETHD for three significant
1064 GMD (see text for details), for two different selective time intervals per GMD. The colored
1065 rings show ETHD increases: between 0-0.1% in ETHD (blue), 0.1% to 0.3% ETHD (orange),
1066 and >0.3% ETHD (red). Black crosses represent ETHD responses which are below the base-line,
1067 or no data. In each panel an additional subpanel is included, showing the time series of the
1068 magnetic field change ($|H'|$, blue line), and a red line marking the point in time corresponding
1069 to that map.

1070

1071

1072



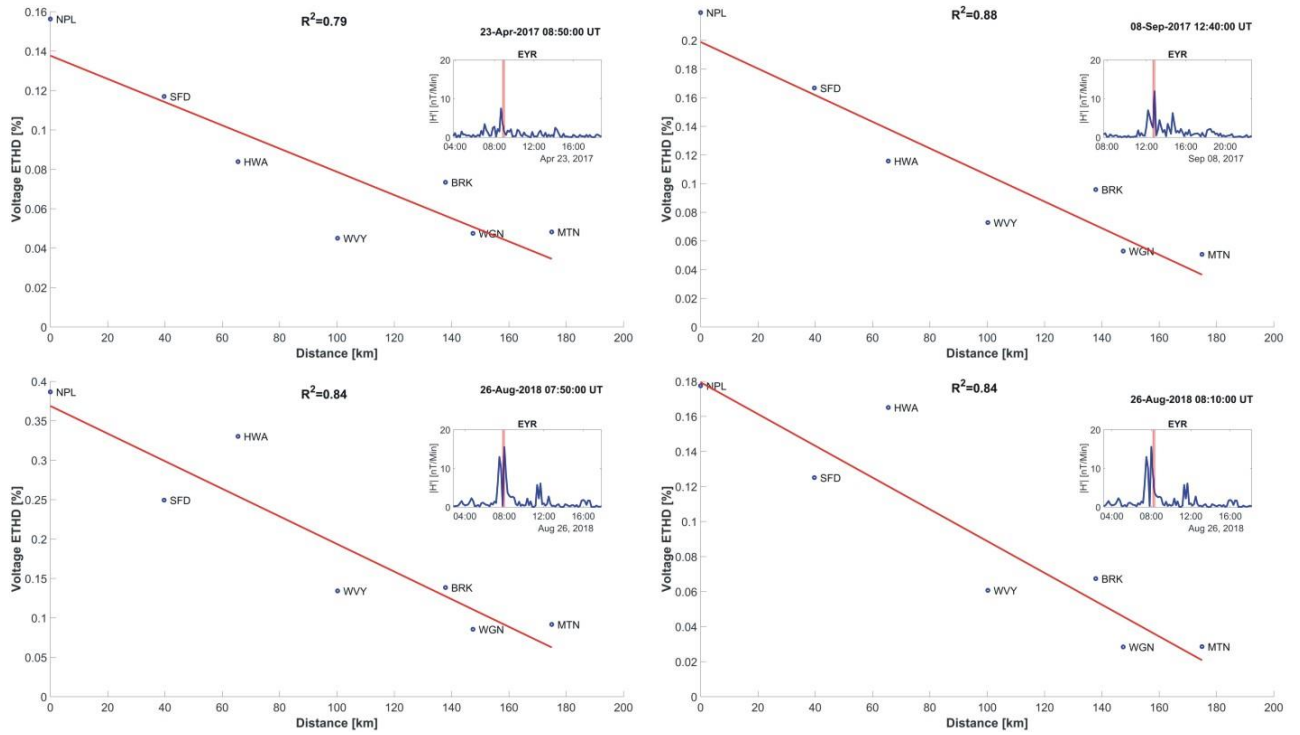
1073

1074 **Figure 4.** Maps showing the electrical transmission lines and substations in regions around
 1075 three of our substations of interest. Substations containing transformers which are earthed
 1076 such that will experience GIC are shown in filled in red circles, effectively un-earthed
 1077 substations are unfilled red circles. Substation locations are marked by their three-letter
 1078 codes. Upper left panel: The mid- and lower North Island region from Taranaki. Upper right
 1079 panel: Tasman/West Coast region of the South Island. Lower panel: The lower South Island.

1080

1081

1082



1083

1084

1085 **Figure 5.** Investigating the decay of GMD-linked ETHD increases in the Taranaki region

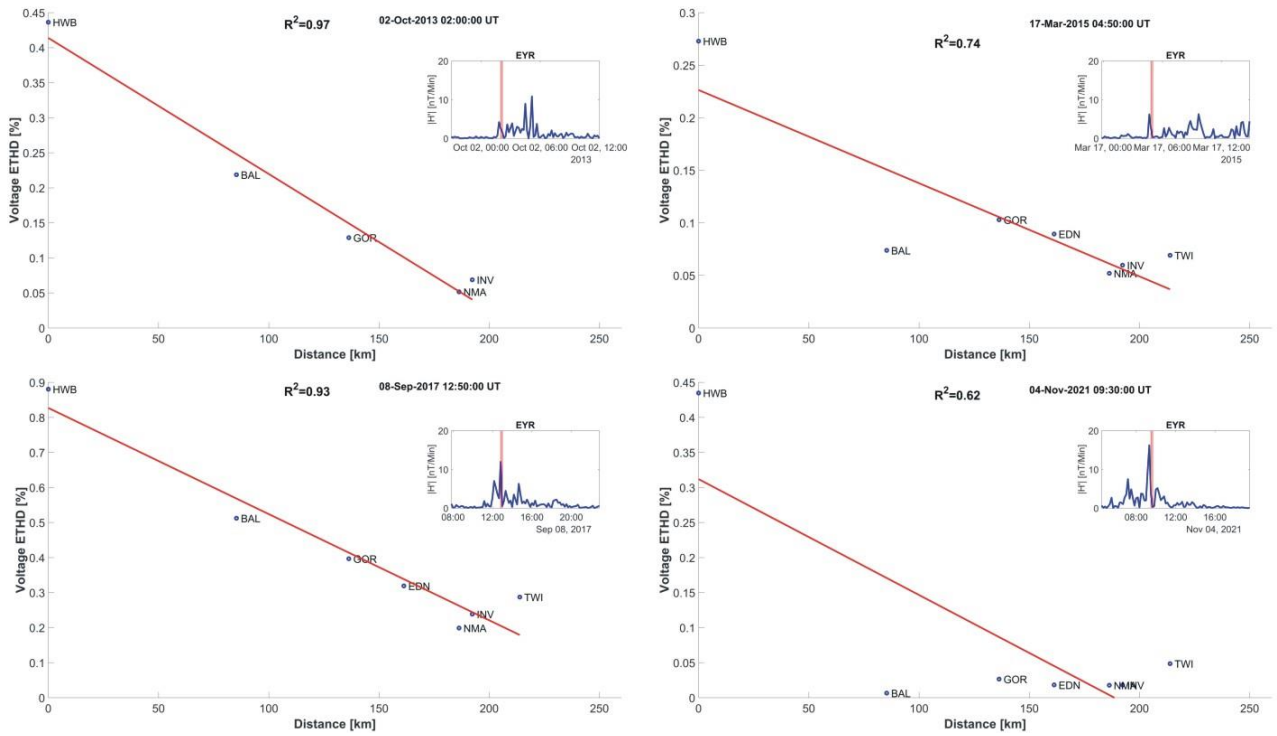
1086 along the transmission line from NPL to MTN (see the maps in Figure 4). We focus on 4 time

1087 periods in 3 different GMD.

1088

1089

1090
1091
1092
1093

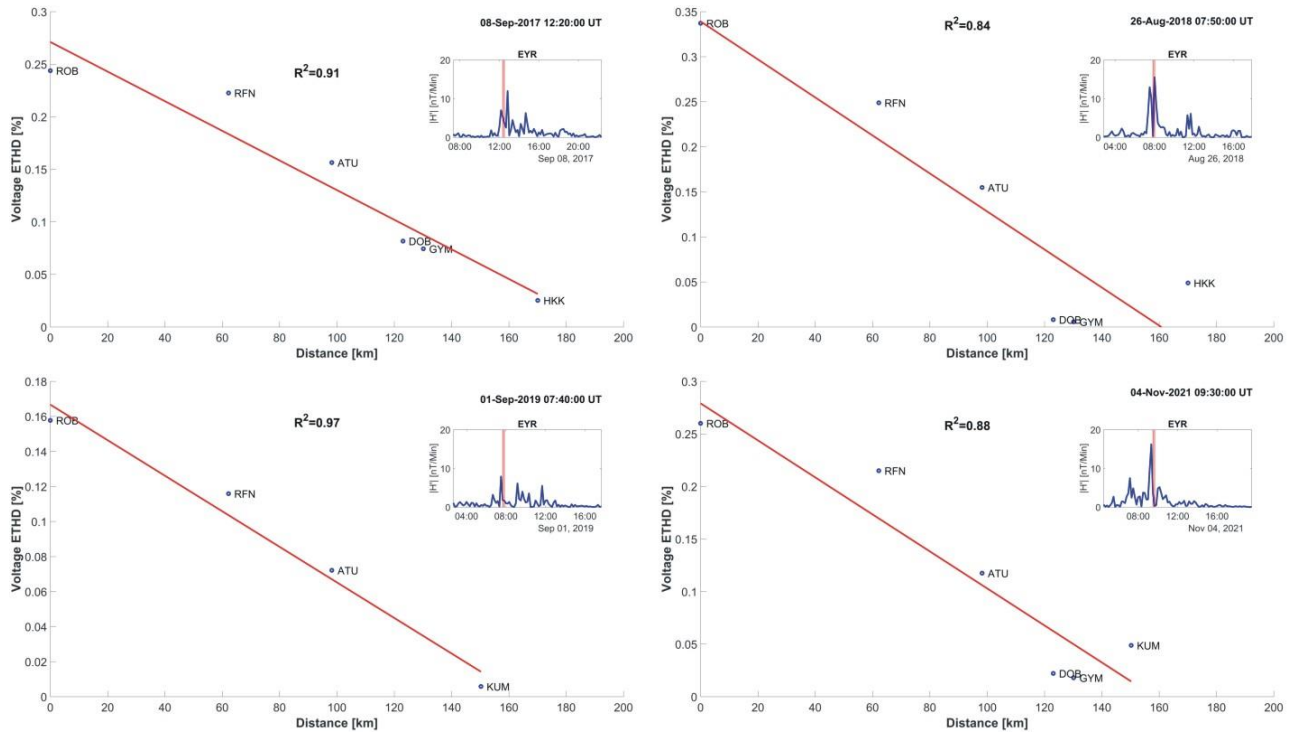


1094
1095
1096
1097
1098
1099

Figure 6. Investigating the decay of GMD-linked ETHD increases in the lower South Island region along the transmission line from HWB southwards towards INV/TWI, showing examples from 4 different GMD.

1100

1101



1102

1103

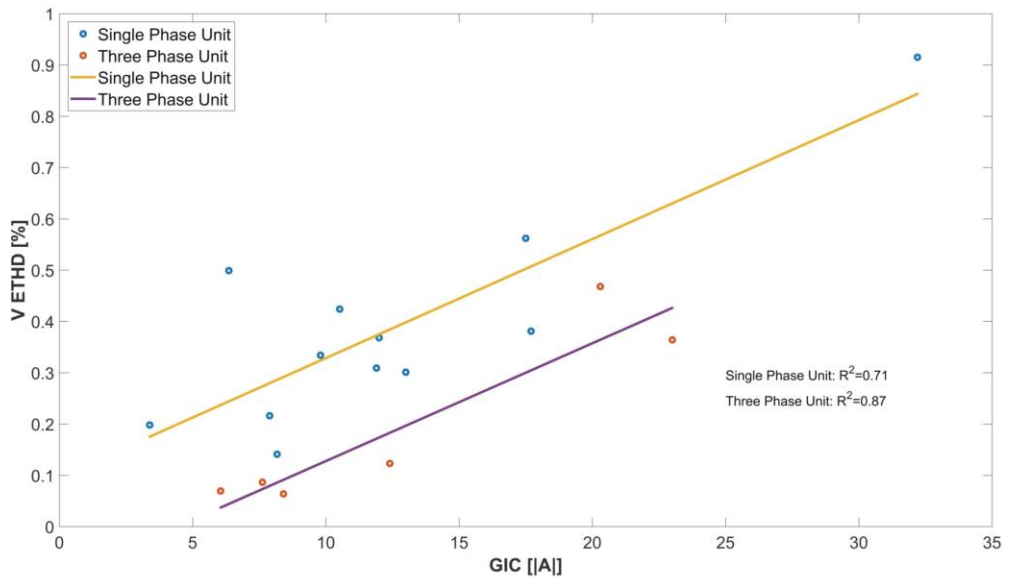
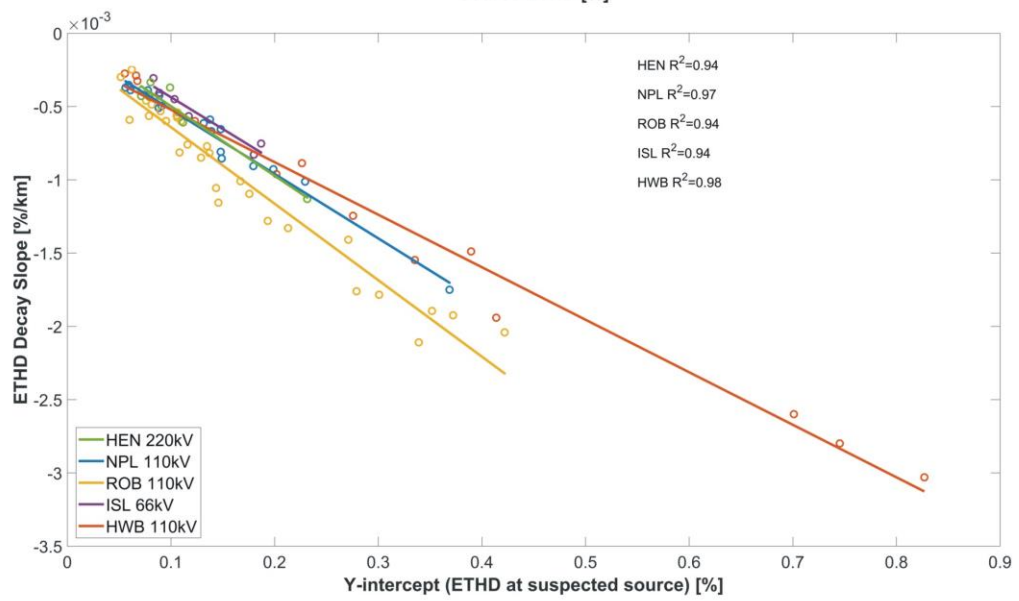
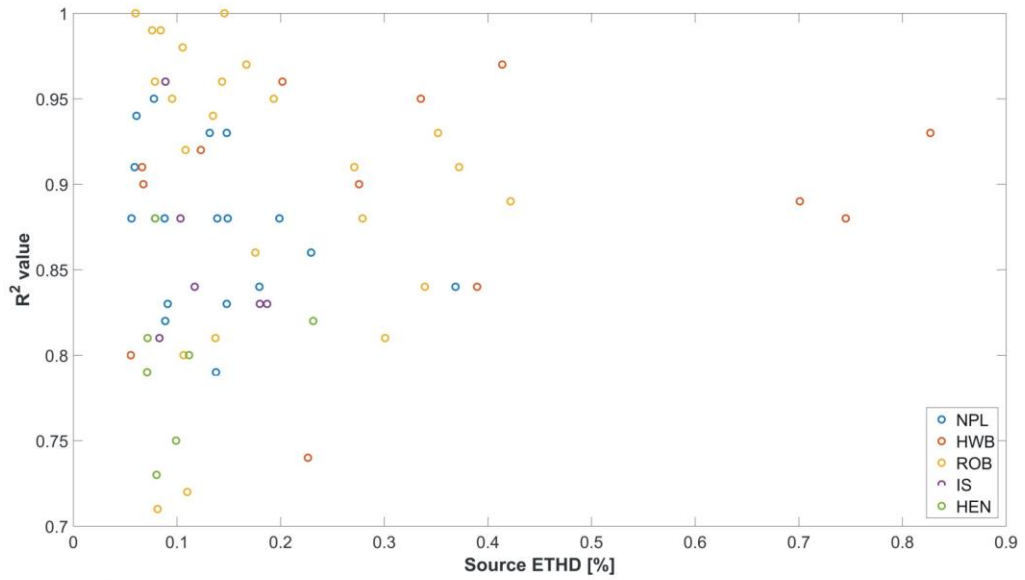
1104

Figure 7. Investigating the decay of GMD-linked ETHD increases on the West Coast of the South Island. Here we focus on increases which may come from the ROB substation, looking at substations to the south. Examples are presented from 4 different GMD.

1107

1108

1109



1110
1111

1112 **Figure 8.** Further examination of ETHD propagating from the identified source substations.
1113 Upper panel: quality of the fitted linear decay against the magnitude of the ETHD produced
1114 at the suspected source substation. Middle Panel: Comparison of the fitted ETHD decays with
1115 distance depending on ETHD at the source substation. Lower panel: Comparing ETHD
1116 percentages observed at the HWB substation depending on GIC magnitude, before and after
1117 the HWB T4 unit was decommissioned in late November 2017.
1118

Figure 1.

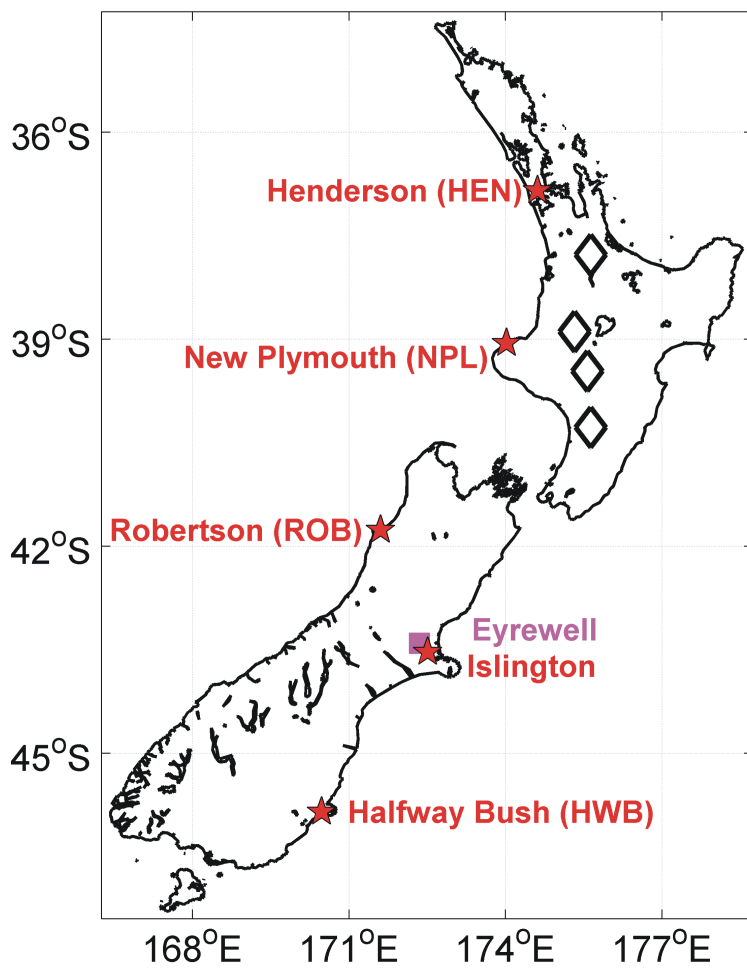
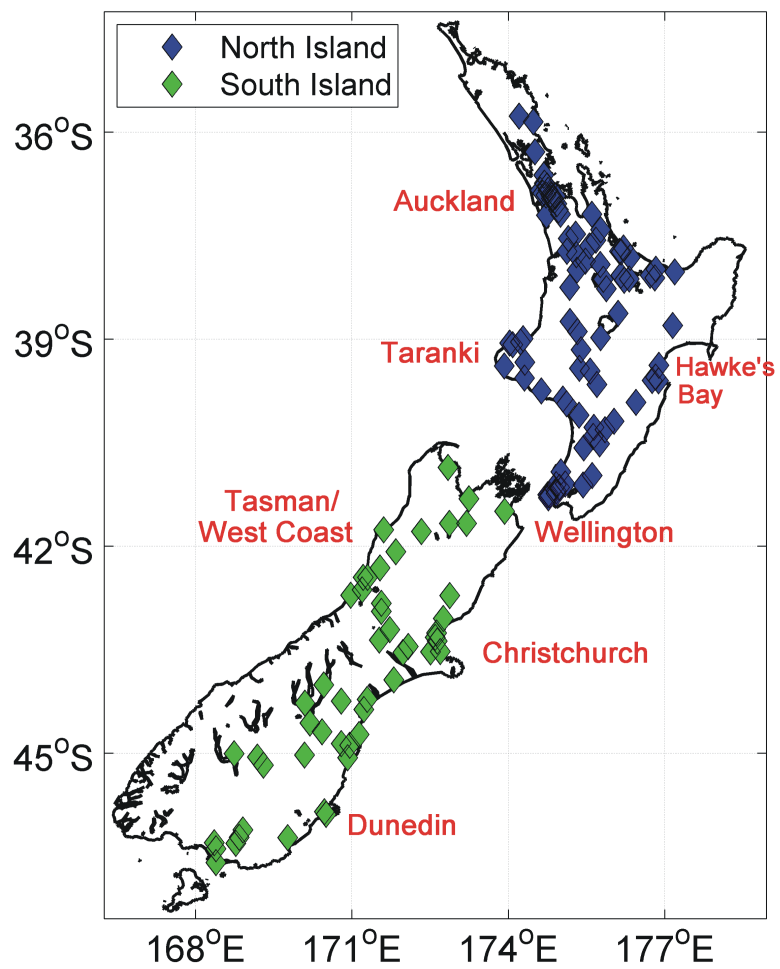


Figure 2.

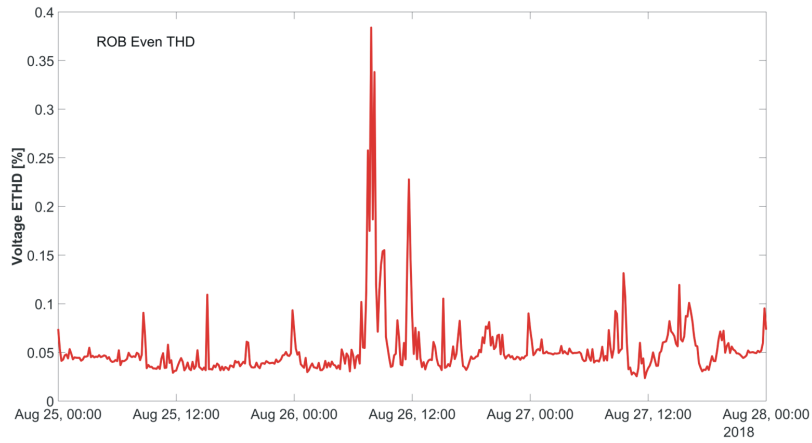
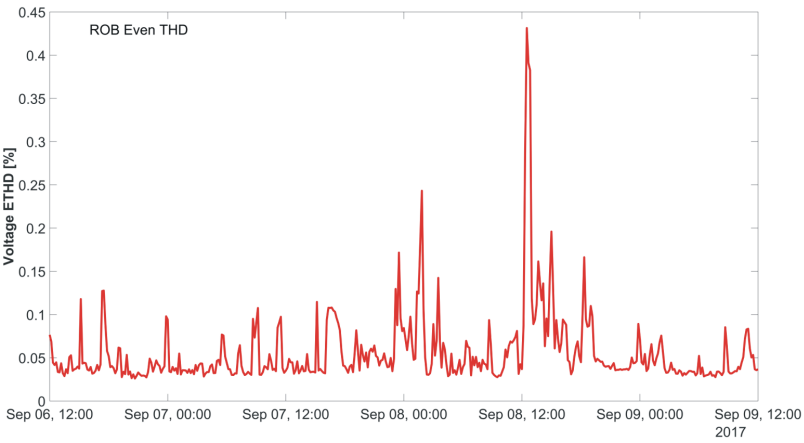
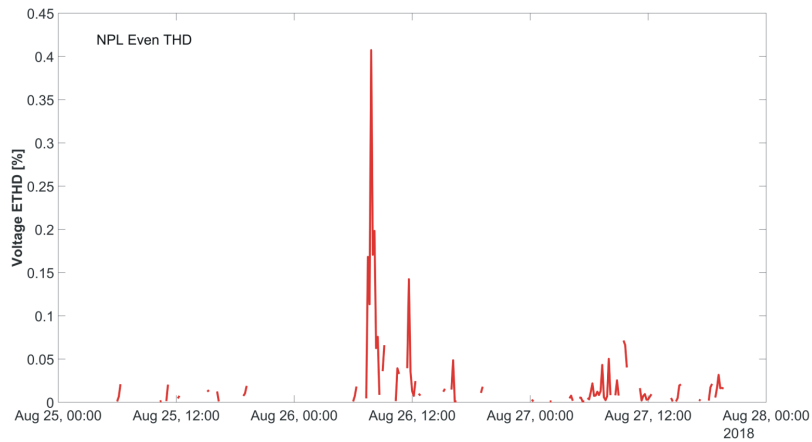
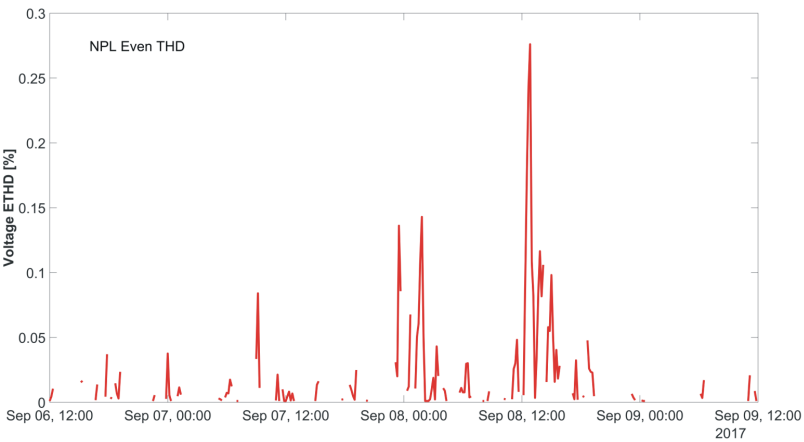
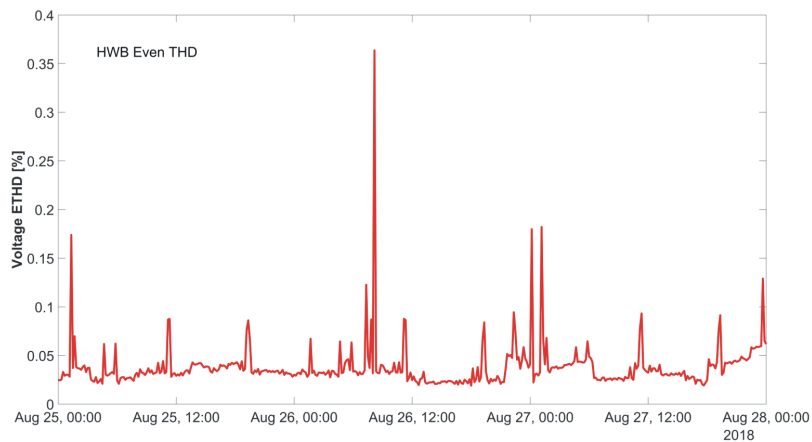
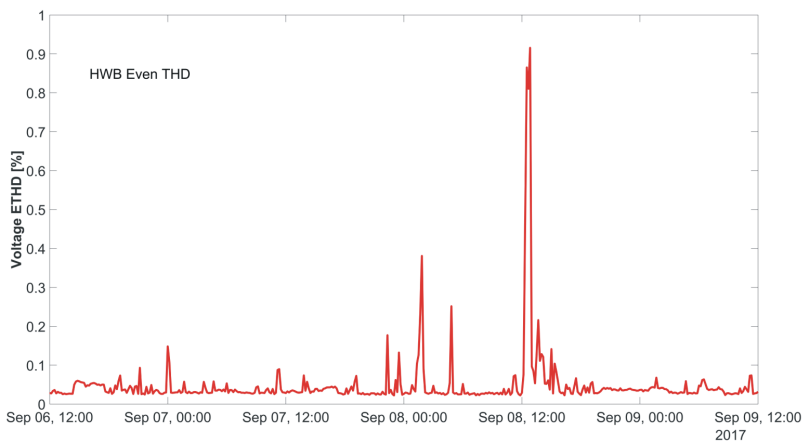
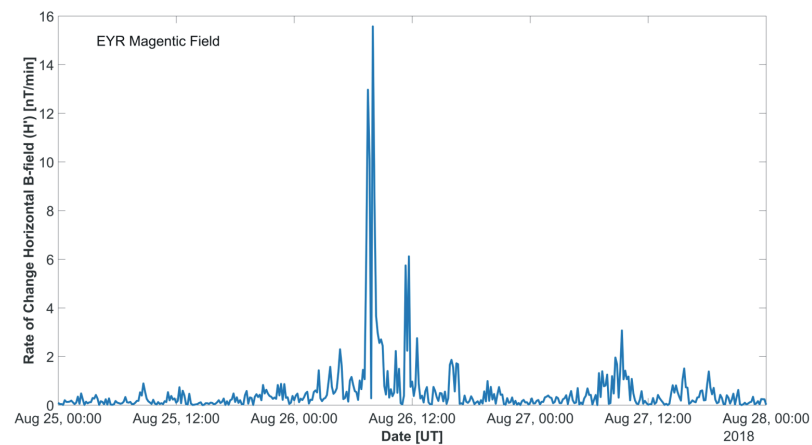
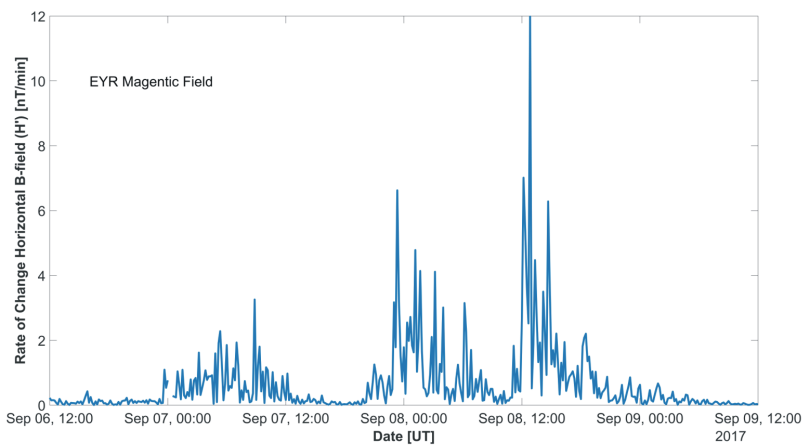


Figure 3.

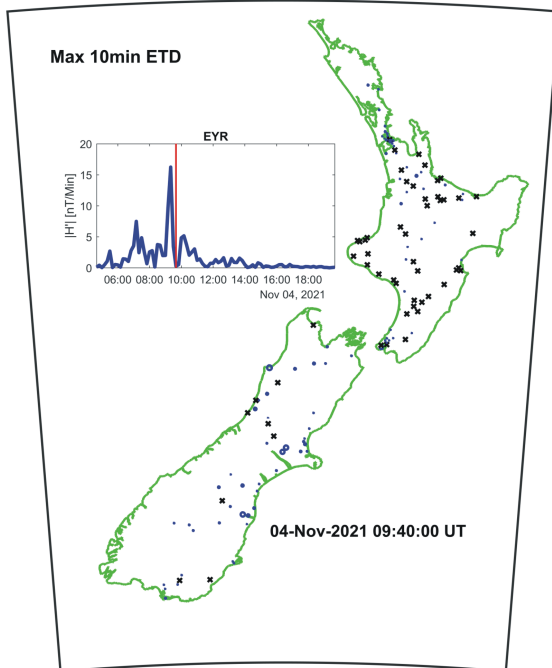
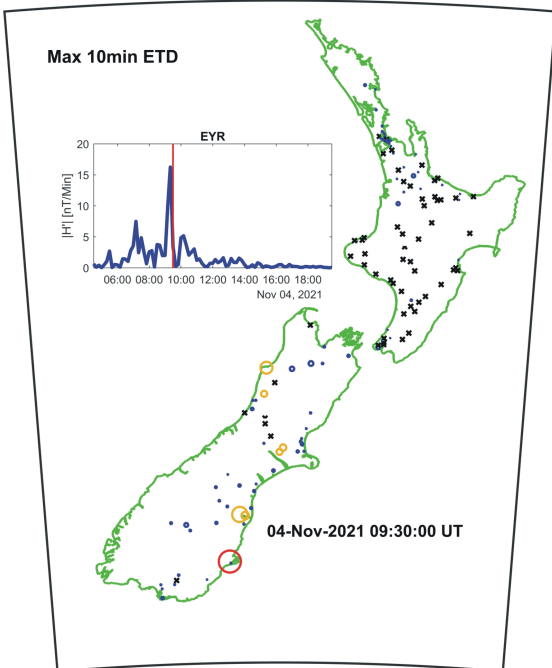
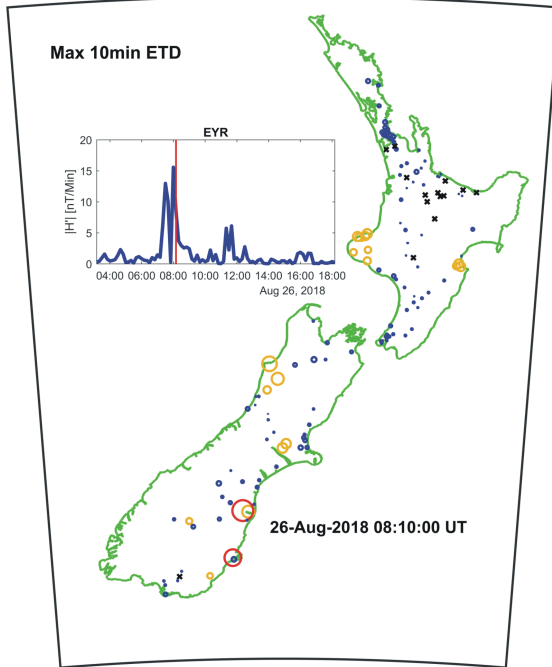
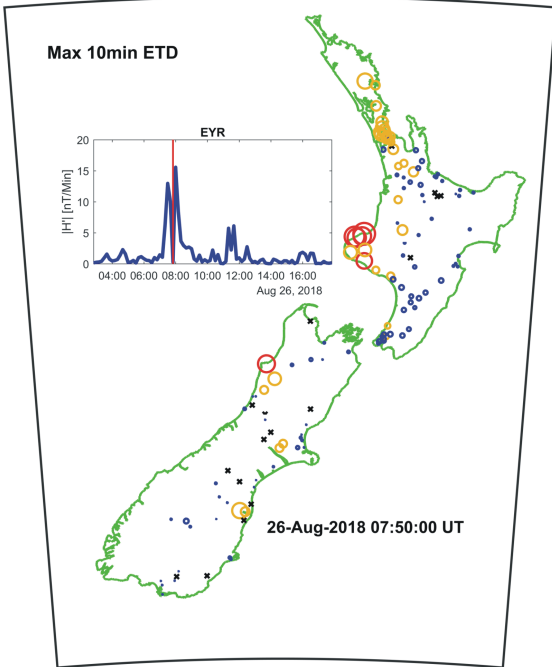
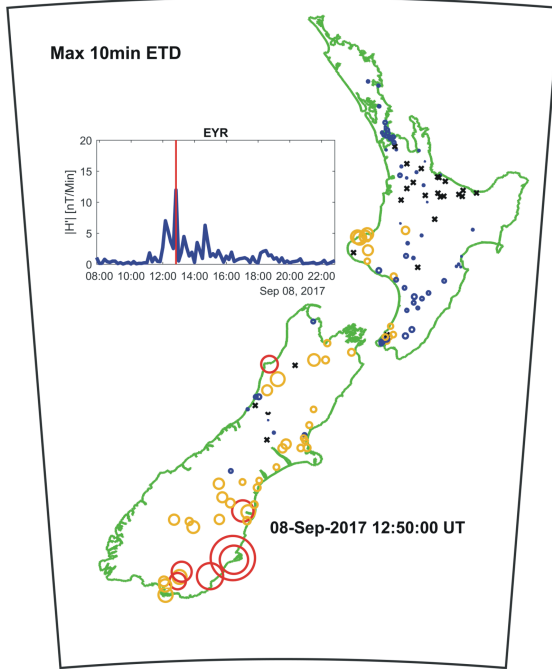
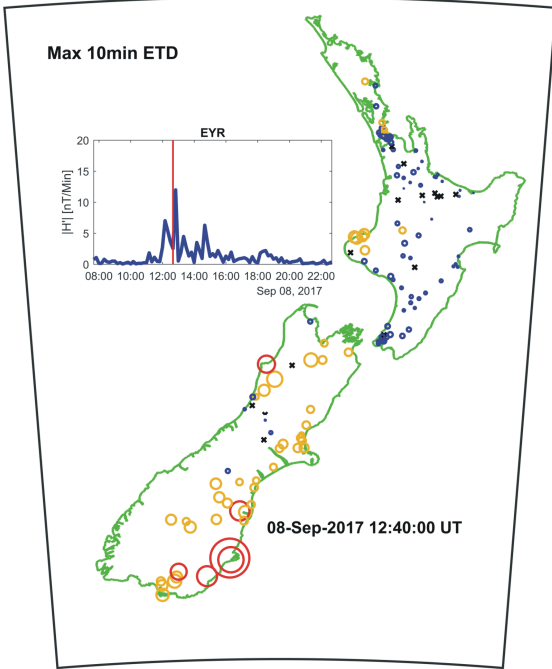


Figure 4.

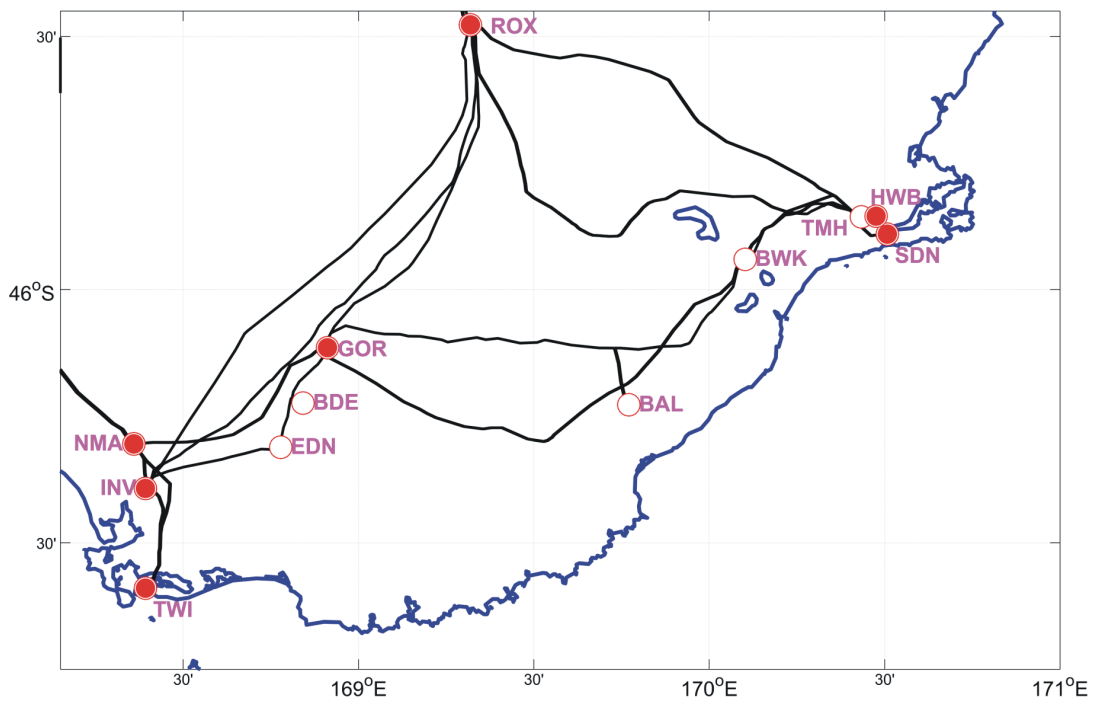
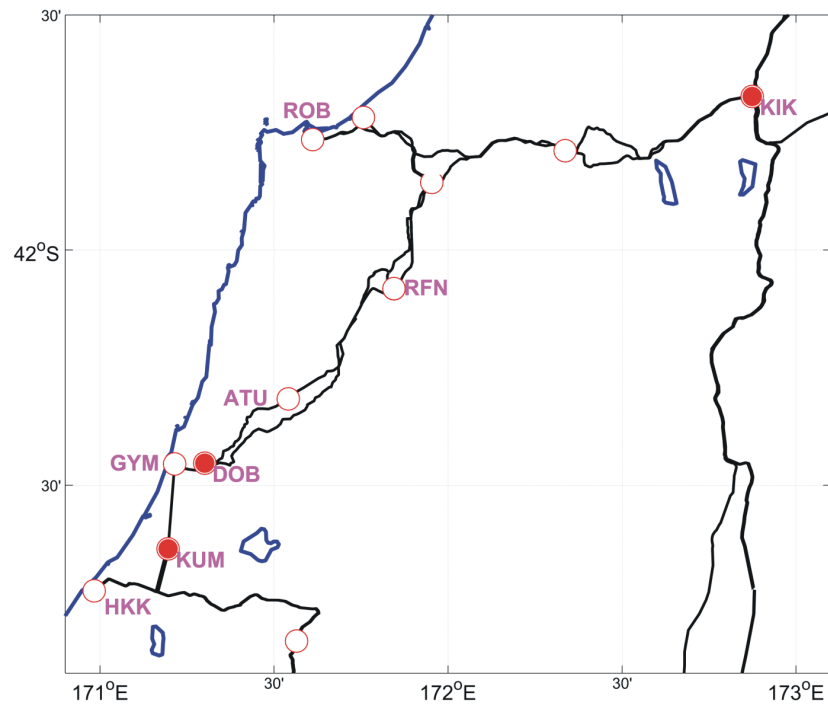
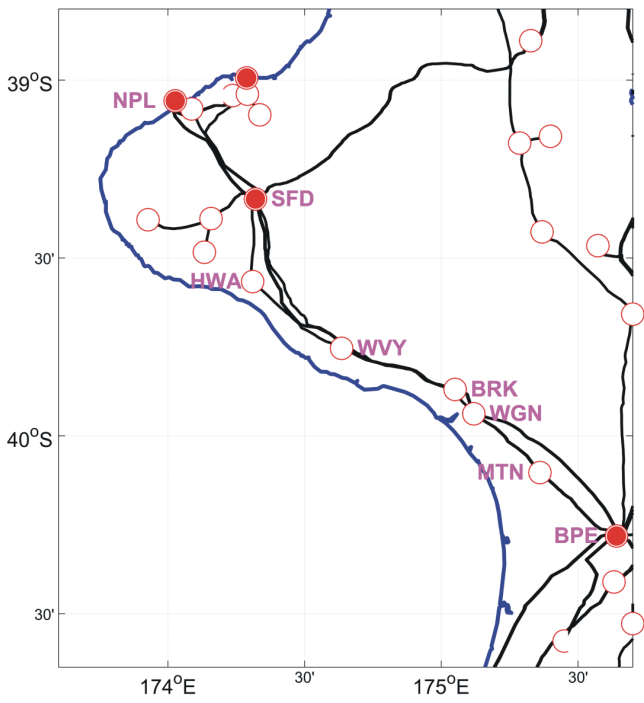


Figure 5.

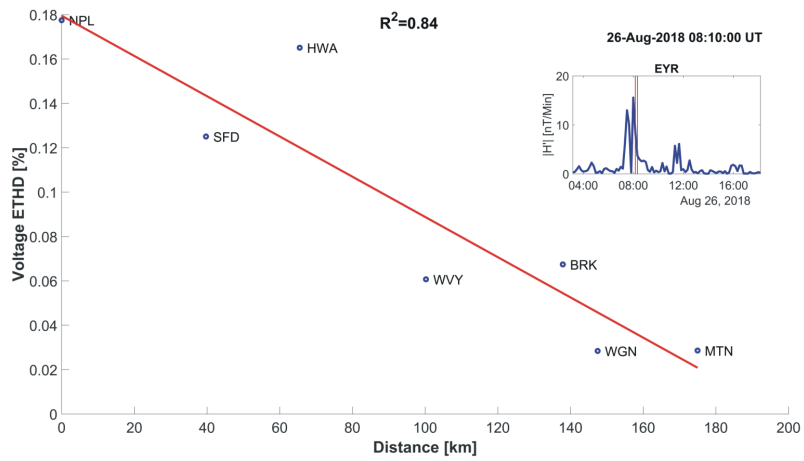
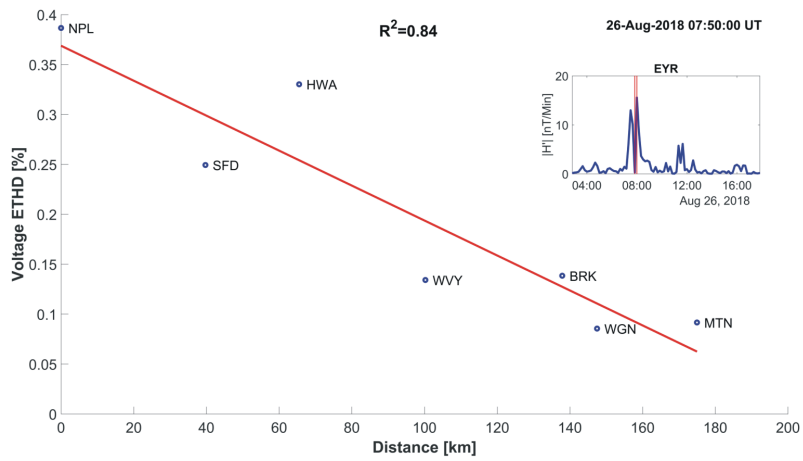
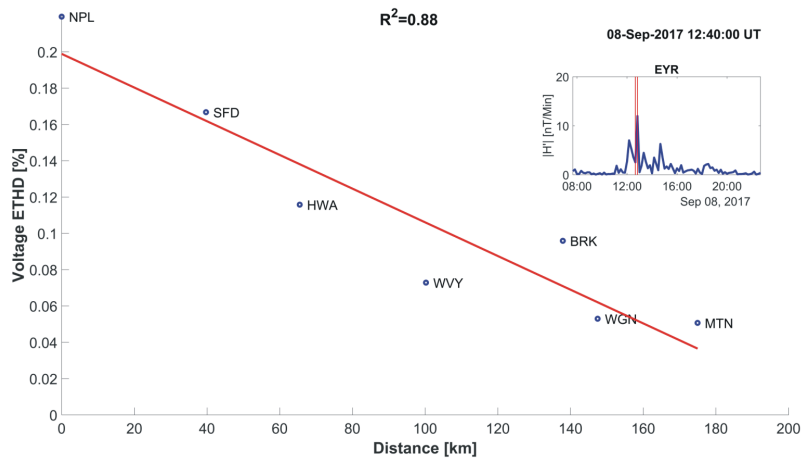
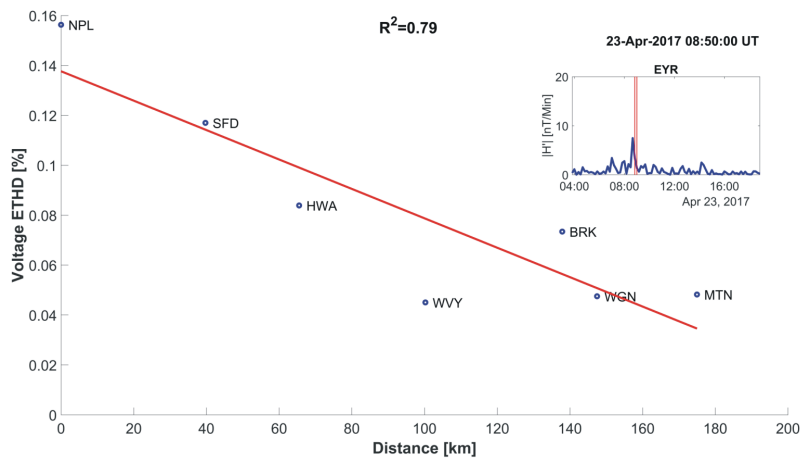


Figure 6.

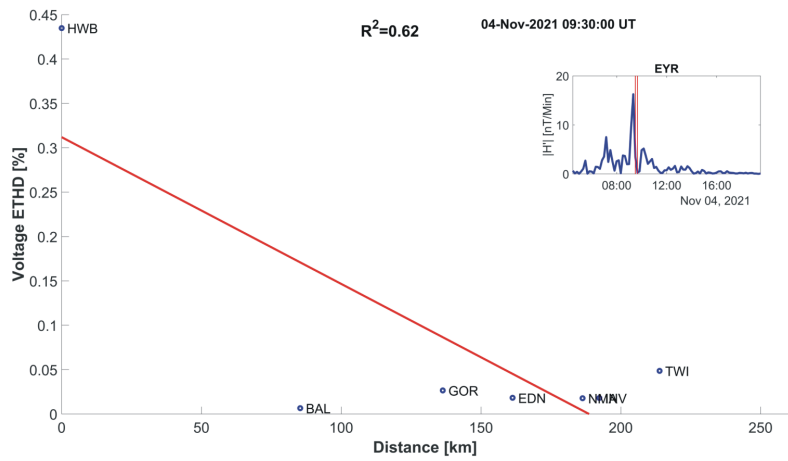
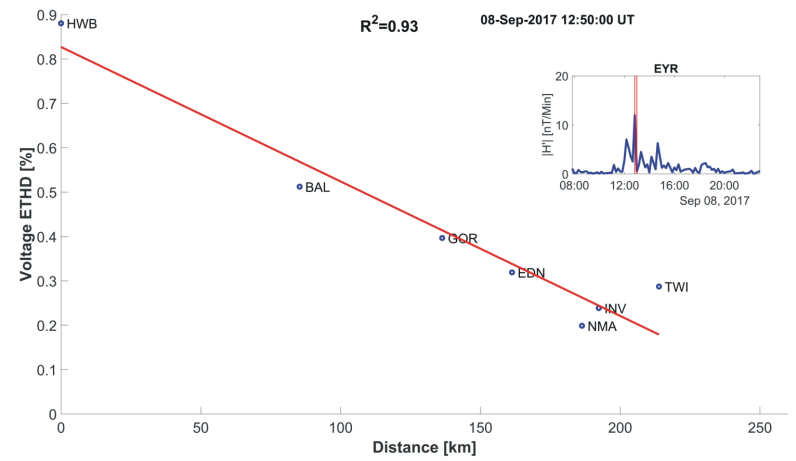
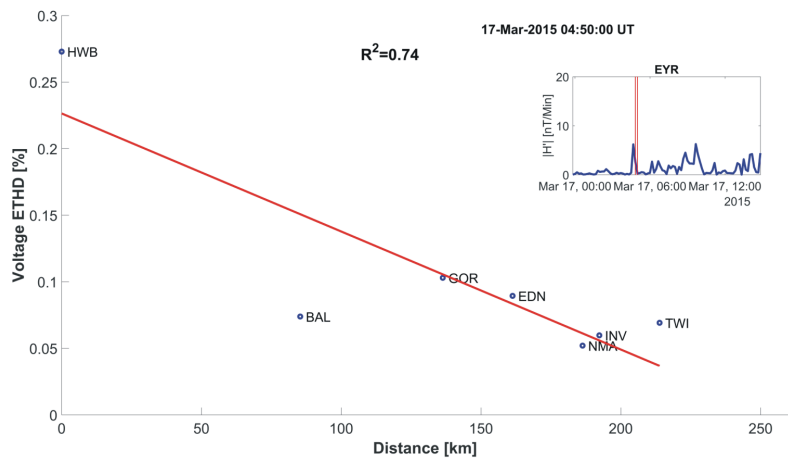
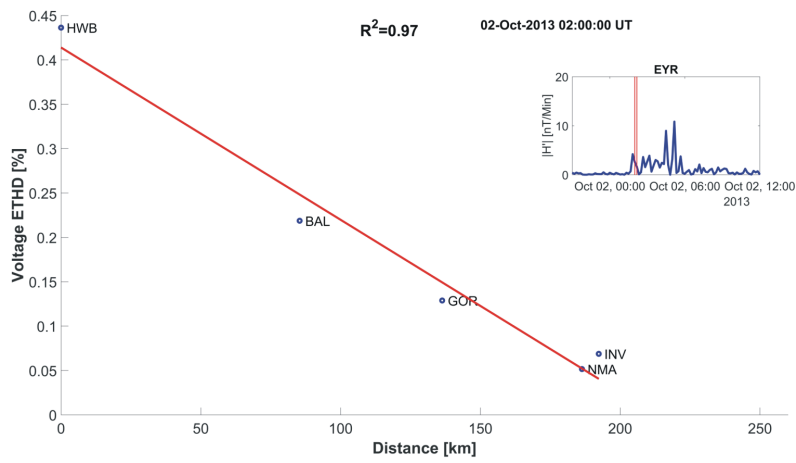


Figure 7.

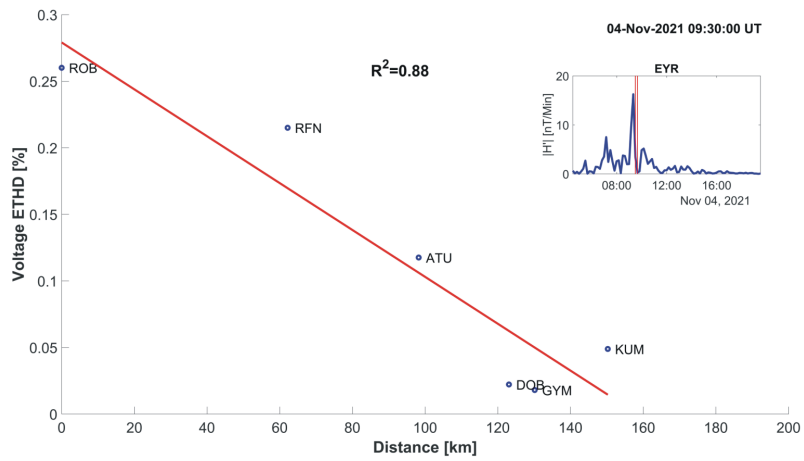
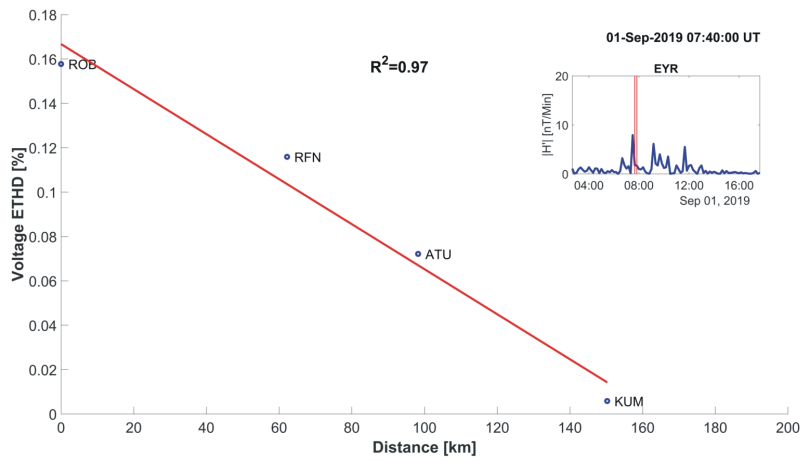
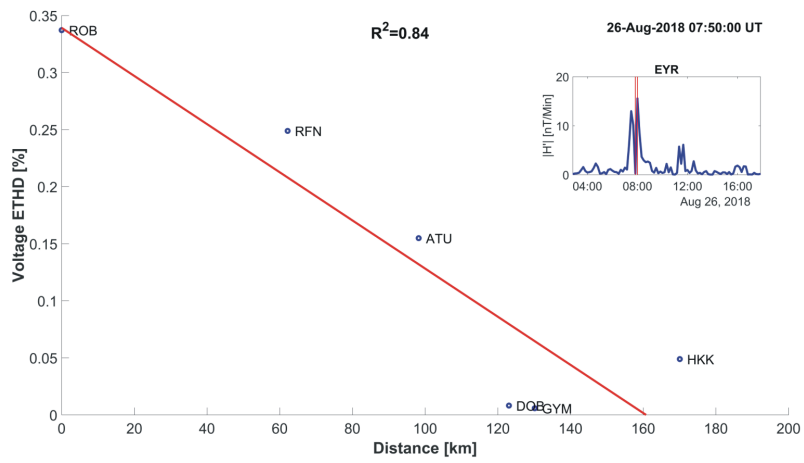
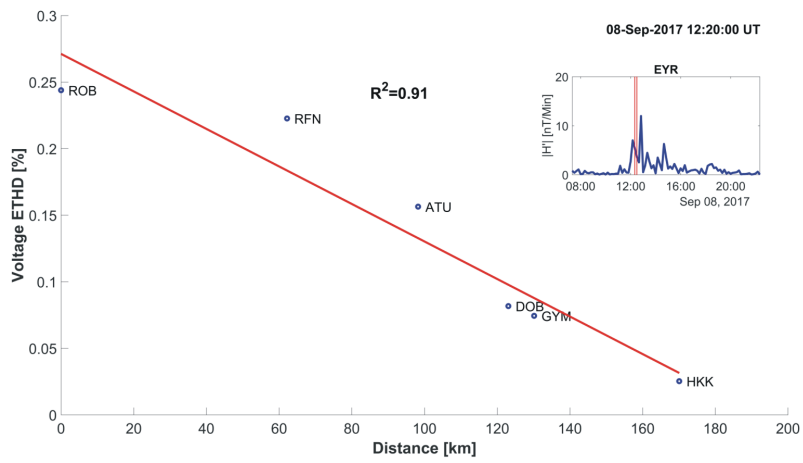


Figure 8.

